ON A UNIFORM GEOMETRICAL OPTICS ANALYSIS VALID ACROSS SMOOTH CAUSTICS OF RAYS REFLECTED BY SMOOTHLY INDENTED BOUNDARIES

P.H. Pathak and M.C. Liang

The Ohio State University

ElectroScience Laboratory

Department of Electrical Engineering
Columbus, Ohio 43212

Technical Report No. 716611-3

Contract No. F33615-84-K-1550

July 1987

USAF/AFSC

Aeronautical Systems Division

Wright-Patterson AFB, OH 45433

NOTICES

When Government drawings, specifications, or other data are used for any purpose other than in connection with a definitely related Government procurement operation, the United States Government thereby incurs no responsibility nor any obligation whatsoever, and the fact that the Government may have formulated, furnished, or in any way supplied the said drawings, specifications, or other data, is not to be regarded by implication or otherwise as in any manner licensing the holder or any other person or corporation, or conveying any rights or permission to manufacture, use, or sell any patented invention that may in any way be related thereto.

50272-101

REPORT DOCUMENTATION PAGE	1. REPORT NO.	2.	3. Recipient's Accession No.

4. Title and Subtitle

ON A UNIFORM GEOMETRICAL OPTICS ANALYSIS VALID ACROSS SMOOTH CAUSTICS OF RAYS REFLECTED BY SMOOTHLY INDENTED BOUNDARIES

5. Report Date July 1987

6.

7. Author(s)

P.H. Pathak and M.C. Liang

8. Performing Organization Rept. No 716611-3

9. Performing Organization Name and Address

The Ohio State University
ElectroScience Laboratory
1320 Kinnear Road
Columbus, Ohio 43212

10. Project/Task/Work Unit No.

11. Contract(C) or Grant(G) No

(c) F33615-84-K-1550

(G)

12. Sponsoring Organization Name and Address

USAF/AFSC
Aeronautical Systems Division
Wright-Patterson AFB, Ohio 45433

13. Type of Report & Period Covered Technical

14.

15. Supplementary Notes

16. Abstract (Limit: 200 words)

It is well known that the geometrical optics solution fails at and near ray caustics. It therefore becomes necessary to analyze the fields within ray caustic regions via uniform asymptotic procedures. Uniform asymptotic high frequency expressions are presented here for the fields reflected from both two and three dimensional smoothly curved boundaries, respectively, which are concave, or contain inflection points. These expressions remain uniformly valid across the transition regions adjacent to the smooth caustics of rays reflected in these configurations. While the subject of caustic field analysis is not new, and relatively sophisticated mathematical treatments for evaluating the fields uniformly in caustic regions have become available recently, those solutions do not appear to be readily ammenable for use in practical applications. Other uniform solutions, which also recover the geometrical optics field outside the caustic transition regions on the lit side of the caustic, mostly contain parameters that require a detailed knowledge of the caustic geometry and its location, especially for evaluating the field on the dark side of the caustic. The latter complication is avoided in the present approach. Furthermore, outside the transition region on the dark side of the caustic, the present solution properly reduces to the complex ray field description given recently by Ikuno and Felsen. The present analysis is employed to calculate electromagnetic fields scattered from a concave-convex shaped boundary with an edge as well as by a smoothly idented cavity, each of which contains points of inflection thereby giving rise to smooth caustics of the reflected rays. The accuracy of the numerical results presented for the edged concave-convex boundary is established by comparison with results obtained via an independent moment method analysis.

17. Document Analysis a. Descriptors

b. Identifiers/Open-Ended Terms

c. COSATI Field/Group

18. Availability Statement	19. Security Class (This Report) Unclassified	21. No. of Pages 62
	20. Security Class (This Page) Unclassified	22. Price

(See ANSI-Z39.18) See Instructions on Reverse OPTIONAL FORM 272 (4-77) (Formerly NTIS-35) Department of Commerce

Contents

List of Figures

I Introduction

It is well known that ray optical solutions fail at and near caustics of ray systems thus requiring one to modify the ray solutions in such regions using uniform asymptotic techniques. In this paper, uniform asymptotic high frequency field representations are presented which remain valid within the transition regions adjacent to a smooth caustic formed by the envelope of the geometrical optics (GO) rays reflected from two and three-dimensional smoothly indented perfectly-conducting boundaries in free space. These field representations are uniform in the sense that they are bounded and continuous at the caustic; furthermore, outside the caustic transition regions they recover the GO reflected ray fields which are valid on the lit side of smooth caustics, and they properly reduce to the complex ray fields given recently by Ikuno and Felsen [1] on the dark side of such caustics wherein real rays do not penetrate.

While the subject of evaluating fields in caustic regions is not new, the uniform solutions generally presented in the recent past mainly emphasize the mathematical aspects of the problem; hence, one of the primary goals of this paper is to try to present the uniform results obtained here in a fashion that would be particularly useful for engineering applications requiring a ray analysis of the problems of electromagnetic (EM) scattering by boundaries that can generate smooth caustics of reflected rays. Consequently, an important feature of the present results is that they provide a relatively simple prescription not only for evaluating the fields on the lit side of smooth caustics, but also for evaluating the fields on the dark side of such caustics. It is noted that most other uniform solutions which recover the GO fields

on the deep lit side of the caustic appear to be more complicated for evaluating the fields within and outside the transition region on the dark side of the caustic; this is because the parameters present in those solutions typically must be found from a knowledge of the radius of curvature of the caustic and the perpendicular distance from the caustic to the observation point. While it is known that it also possible to more directly find the parameters in those solutions for the lit side from just a knowledge of the GO fields which need to be corrected within the caustic regions, no such direct simplification appears possible in these solutions to find the parameters for evaluating the fields on for the dark side of the caustic. On the other hand, the parameters occurring in the present solutions can be found relatively easily from the stationary phase points in the physical optics (PO) approximation for the radiation integral over the currents induced on the reflecting boundary by the incident field. It is noted that the PO approximation employs the usual geometrical optics (GO) field to find these induced currents. This PO approximation is valid whenever the smooth reflecting boundary is electrically large and well illuminated; these conditions are assumed to hold in the present analysis and are the same as the ones required in the GO reflection calculations. There are two real stationary phase points in the PO radiation integral over the reflecting boundary for an observation point on the lit side of a smooth caustic of the reflected rays; these stationary points coalesce to form a second order stationary point for observation points on the caustic itself, and then they become two complex stationary points (which are complex conjugates of each other) for observation points on the dark side of the caustic even though only one of these eventually contributes to the fields on the dark side outside the caustic transition region. As usual, the relevant stationary phase points can be

found simply by requiring the spatial derivatives of the phase function in the PO radiation integral over the reflecting surface to vanish as described later in Section II.

It is useful at this juncture to briefly review some of the previous related work. Rahmavard and Rusch [2] treated the problem of electromagnetic (EM) scattering by a shaped subreflector surface with a point of inflection. Their PO based asymptotic solution is valid in the transition region adjacent to the locally smooth portion of the reflected ray caustic which results from the effect of an inflection point on the subreflector geometry. However, their solution is only partially uniform as it does not recover the GO reflected field on the lit side of the caustic; also, they introduced an additional approximation in the asymptotic treatment of the PO radiation integral for evaluating the field on the dark side of the caustic instead of making use of the complex stationary points in the integrand. Nevertheless, their solution provided some useful numerical results for shaped subreflector design when it was employed within its range of validity. Albertsen, et al. [3] obtained a solution valid near smooth caustics of edge diffracted rays; they performed an asymptotic evaluation of the radiation integrals over equivalent edge currents to arrive at their solution. Next, they introduced a heuristic factor in their solution so that the resulting modified solution would reduce uniformly to the ray solution (based on Keller's edge diffracted ray fields) on the lit side of the caustic; they also introduced the same approximation as in [2] for the dark side of the caustic. Kravatsov [4], and Ludwig [5], independently showed that the leading terms of an asymptotic solution which remained uniformly valid across a smooth caustic contained not just an Airy function as in [2,3], but also its derivative which was missing in [2,3]. Ludwig's

ansatz [5] is actually based on a uniform asymptotic evaluation of an integral with two nearby saddle points as given by Chester, Friedman and Ursell [6]. The latter asymptotic evaluation is summarized lucidly in texts by Felsen and Marcuvitz [7], and Stamnes [8]. While the term involving the derivative of the Airy function vanishes at the caustic, it is of the same order as the Airy function term exterior to the caustic transition region and its inclusion is therefore necessary to uniformly recover the corresponding ray solution deep in the lit region. It is noted that the solutions developed in this paper also contain the Airy function and its derivative since the integrals leading to these solutions are evaluated asymptotically using the techniques developed by Chester, et al. [6,7]. Ludwig's analysis [5] provides important extensions to the earlier work of Kay and Keller [9], and in particular of Buchal and Keller [10]. Ludwig's approach [5] requires one to initially assume a general form of the uniform solution given by Chester, et al. [6] and the amplitudes and arguments of the uniform functions (involving the Airy function and its derivatives) are then obtained by requiring the solution to satisfy the wave equation in the high frequency limit. However, this systematic and elegant approach for the two-dimensional case by Ludwig [5] appears to be cumbersome especially for treating the corresponding three-dimensional case. More recently, phase-space techniques have been employed by Maslov [11,12] for evaluating the fields in the neighborhood of ray caustics; in that method, the field is eventually expressed as a spectral integral which can be transformed locally into a canonical form, as, for example, the one treated by Chester, et al. [6] for the case of a smooth caustic. The general relationships between caustics, their associated field singularities and ray geometries are also expressed in a systematic fashion in catastrophe theory [13], which defines

caustics as singularities of ray families and classifies caustics according to their singularities. In particular, the smooth caustic is classified as a "fold" catastrophe. Catastrophe theory provides a mapping for the phase function in an integral representation for the field near a caustic so that it can like wise be locally transformed into a canonical integral. Very recently, Arnold [14,15] has essentially extended Maslov's method to include discontinuities in a scattering boundary; there, he employs a spectral synthesis of uniform wavefunctions for analyzing fields near smooth caustics based on ideas common to Maslov's method and catastrophe theory. As in the present approach, Arnold's method is readily applicable to treat the case of smooth caustics in three dimensions. However, even though these previous elegant treatments in [4]-[6],[10]-[15] provide the general concepts involved for analyzing the fields in caustic regions, they are presented at a relatively sophisticated mathematical level and the final solutions which generally avoid any explicit treatments of the fields on the dark side of the caustic do not appear to be readily ammenable for use in engineering applications. These treatments in [4]-[6],[10]-[15] provide uniform solutions (usually explicitly for the lit side of the caustic) which contain parameters that are essentially expressed in terms of the caustic (or corresponding wavefront) geometry; hence, it is necessary first to know the details of the caustic geometry especially for evaluating the fields on the dark side of the caustic. The latter complication is avoided in the present approach. It is noted that the present approach can be easily generalized to deal with the reflection from an impedance boundary or from a dielectric interface.

The problems of two and three-dimensional smooth caustics are analyzed in essentially the same fashion in the present approach. If there are two caustics, the present analysis is valid across each caustic provided that the obervation point is far from the region where the two caustics merge together to from a cusp. Near the cusp, a different approximation is necessary. There are generally two smooth caustics present in the (3-D) case; the present analysis is valid across each smooth caustic for the latter case provided that these two caustic surfaces do not intersect. In practical applications, the surfaces which scatter are of finite extent; hence, there may be situations where the caustic can terminate in which case the present analysis is valid across a locally smooth portion of the caustic which is sufficiently far from the caustic termination, and the generally smaller effect of that termination must be found separately. The uniform results are developed and presented here in Sections II and III for the 2-D and 3-D vector EM cases, respectively, with all the parameters being defined explicitly for both the lit and the dark side of the caustics in a form suitable for engineering applications. These uniform results are employed in this paper to analyze the scattering by boundaries which contain inflection points. In particular, numerical results have been obtained, as shown in Section IV, for the far zone EM plane wave backscattering by a concave-convex shaped boundary with an edge, and also by a smoothly indented cavity, both of which contain points of inflection on their boundaries. The numerical results for the concave-convex geometry with an edge are shown to compare well with independent moment-method calculations. Numerical results for the smoothly indented cavity are compared with those of a rectangular cavity of the same length and depth. It is seen that the scattering from the smoothly indented cavity can be of the same order

within the caustic regions as that from a non-smooth rectangular shaped cavity.

An e^{jwt} time dependence is assumed and suppressed in the following analysis.

II An Asymptotic Solution for the Field Associated with a Two Dimensional Smooth Caustic

An asymptotic high frequency analysis is presented in this section for predicting the EM fields within the caustic regions of rays reflected from smoothly indented perfectly-conducting two dimensional boundaries in free space. The excitation in these problems is assumed to be produced by a localized source which is sufficiently far (in terms of the electrical wavelength) from the boundaries so that the field incident from the source can be represented ray-optically. If the excitation is due to an electrically large or extended source distribution, then one can quantize that source distribution so that each quantized source element satisfies the above criterion; the complete reflected field in this case can be found by a superposition of the fields reflected from the boundaries when they are illuminated by each of the quantized source elements.

The scattering by geometries depicted in Figures 1(a) and (b) represent typical situations of interest here in which smooth caustics of reflected rays are formed. Both the non-uniform as well as the uniform asymptotic high frequency approximations of the physical optics integral for the scattered field in two-dimensions are presented separately in Parts A and B of this section, respectively. The non-uniform asymptotics furnish the usual pair of GO reflected ray fields on the lit side of the smooth caustic of reflected rays; these two real reflected rays are associated with the two real stationary phase points in the PO integrand, and they become degenerate as the stationary points coalesce for observation points on the caustic where their associated field exhibits a singularity. The non-uniform asymptotics also provides

a result for the field on the dark side of the caustic which is associated with only one of the two complex stationary points; as indicated earlier by Ikuno and Felson [1], this evanescent (exponentially decaying) field can be described in terms of a complex ray specularly reflected from a complex extension of the surface. The other complex (conjugate) stationary point gives an unbounded result and it must be discarded in the non-uniform analysis on physical grounds as its contribution violates the radiation condition. The non-uniform result for the dark side also exhibits a field singularity at the caustic as does the GO result for the lit side. It is for the sake of completeness that the non-uniform asymptotic treatment is included; moreover, it serves to introduce the notation which is also used later in the uniform asymptotic analysis. Of course, the non-uniform result is not valid at and near the caustic; instead, one must employ a uniform solution there as discussed in Part B.

II-A Non-Uniform 2-D Analysis:

The electric field $\bar{E}^s(P)$ at any point P exterior to the boundary C of Figures 1(a) and 1(b) which here constitutes the field scattered by the boundary can be expressed in terms of the usual radiation integral over the electric current $\bar{J}$ induced on C by the source at P' as

$$\bar{E}^s(P) \approx \frac{kZ_o}{4} \int_C [\hat{R} \times \hat{R} \times \bar{J}(Q')]\, H_o^{(2)}(kR) d\ell_1' \qquad (1)$$

where $\bar{J}(Q')$ is the value of $\bar{J}$ at any point Q' on the boundary C and $\bar{R} = \overline{Q'P}$. Also, the point P cannot be too close to the reflecting boundary for (1) to be valid. Also k and Z_o are the wavenumber and impedance of free space respectively and $H_o^{(2)}(kR)$ is the usual cylindrical Hankel function of the second kind of order zero.

To be specific, $P = P_L$ for an observation point on the lit side of the caustic and $P = P_S$ for an observation point on the dark side of the caustic, respectively. In the PO approximation to (1), the $\bar{J}(Q')$ is assumed to be given by GO as follows:

$$\bar{J}(Q') \approx \begin{cases} 2\hat{n} \times \bar{H}^i(Q'), \text{ on the lit portion of the boundaries} \\ 0, \text{ on the shadowed portion of the boundaries} \\ \quad \text{(where the direct illumination from the source is absent)} \end{cases}, \quad (2)$$

in which $\bar{H}^i(Q')$ is the magnetic field at Q' which is directly incident from the source whose phase center is at P', and $\hat{n}$ is the unit normal vector to the boundary C at (Q') as shown in Figures 1(a) and 1(b). Under the previously mentioned assumptions, the $\bar{H}^i(Q')$ may be expressed ray optically as

$$\bar{H}^i(Q') \sim Z_o^{-1}\, \hat{s}^i \times \bar{A}\, \frac{e^{-jks^i}}{\sqrt{s^i}} \text{ ; with } \hat{s}_o^i \cdot \bar{A} = 0 \quad (3)$$

It is also understood that $\bar{H}^i(Q') \approx Z_o^{-1} \hat{s}^i \times \bar{E}^i(Q')$, in which $\bar{s}^i = \overline{P'Q'}$, $\hat{s}^i = \frac{\bar{s}^i}{|\bar{s}^i|}$, and $\bar{E}^i(Q')$ is the electric field associated with $\bar{H}^i(Q')$; it is clear from (3) that $\bar{E}^i(Q') = \bar{A}\frac{e^{-jks^i}}{\sqrt{s^i}}$. Using the large argument approximation of $H_o^{(2)}(kR)$ for $kR >> 1$, and the assumed current in (2) within (1) yields the PO integral for $\bar{E}^s(P)$ at an observation point P as

$$\bar{E}^s(P) \approx \sqrt{\frac{jk}{2\pi}} \int_C [\hat{R} \times \hat{R} \times (\hat{n} \times \hat{s}^i \times \bar{A})] \frac{e^{-jk(s^i+R)}}{\sqrt{s^i R}}\, d\ell_1' \quad (4)$$

The integral in (4) can be evaluated for large k via the method of stationary phase [7,8]. The stationary phase points are determined by the condition

$$\hat{\ell}_1' \cdot \nabla(s^i + R) = 0 \quad (5)$$

in which $\bar{d}\ell_1' = \hat{\ell}_1' d\ell_1'$ along the two-dimensional reflecting boundary C. Both s^i and R are functions of ℓ' (arc length to Q' along C from some reference point O on C). The solution to (5) yields the stationary phase points at:

$$\ell_1' = \begin{cases} \ell_{1a}' \text{ and } \ell_{1b}' \text{ , at } Q_a \text{ and } Q_b \quad \text{respectively on C,} \\ \text{when } P = P_L \text{ for an observation point on the lit side of the caustic} \end{cases} \tag{6}$$

where for the sake of being specific one requires the following, in addition to (5):

$$\left.\frac{\partial^2(s^i + R)}{\partial \ell_1'^2}\right|_{\ell_1' = \ell_{1a}'} > 0 \; ; \; \left.\frac{\partial^2(s^i + R)}{\partial \ell_1'^2}\right|_{\ell_1' = \ell_{1b}'} < 0 \; ,$$

and

$$\ell_1' = \begin{cases} \ell_{1a}^c \text{ and } \ell_{1b}^c, \text{ at } Q_a^c \text{ and } Q_b^c \text{ respectively,} \\ \text{when } P = P_L \text{ for an observation point on the dark side of the caustic.} \end{cases} \tag{7}$$

The points Q_a^c and Q_b^c are associated with the complex stationary phase points ℓ_a^c and ℓ_b^c which are conjugates of each other; thus, Q_a^c and Q_b^c must lie on the complex extension of the boundary C as indicated in [1]. At the stationary points which correspond to points of specular reflection at Q_a and Q_b on C, for $P = P_L$, the following conditions hold; namely:

$$\hat{R} \times \hat{n} = \hat{s}^i \times \hat{n} \; ; \tag{8}$$

$$\hat{R} \cdot \hat{n} = -\hat{s}^i \cdot \hat{n} \equiv \cos\theta^i \tag{9}$$

$$\hat{R} - \hat{s}^i = 2(\hat{n} \cdot \hat{R})\hat{n} = 2\cos\theta^i \hat{n} \tag{10}$$

$$\hat{R} = \hat{s}^r_{a,b} \quad \text{for } Q' = Q_{a,b} \tag{11}$$

$$\hat{s}^i = \hat{s}^i_{a,b} \quad \text{for } Q' = Q_{a,b}$$

$$\hat{n} = \hat{n}_{a,b} \quad \text{for } Q' = Q_{a,b}$$

$$\theta^i = \theta^i_{a,b} \quad \text{for } Q' = Q_{a,b}$$

In the neighborhood of the stationary points Q_a and Q_b when $P = P_L$, one arrives at the following local approximation for the phase term $k(s^i + R)$ as:

$$s^i + R \approx s^i_{a,b} + s^r_{a,b} + \frac{1}{2} G_1(Q_{a,b}) \cos^2 \theta^i_{a,b} (\ell'_1 - \ell'_{1a,1b})^2 \quad , \quad \text{for } Q' \quad \text{near} \quad Q_{a,b} \quad . \tag{12}$$

At high frequencies; i.e., for large k, the dominant contribution to (4) comes from the stationary phase points Q_a and Q_b on C when $P = P_L$; thus, (4) may be approximated via (12) as usual to obtain:

$$\begin{aligned} \bar{E}^s(P_L) \approx \sqrt{\frac{jk}{2\pi}} \Bigg\{ & [\hat{R}_a \times \hat{R}_a \times (\hat{n}_a \times \hat{s}^i_a \times \bar{A}(Q_a))] \frac{e^{-jk(s^i_a + s^r_a)}}{\sqrt{s^i_a s^r_a}} \\ & \cdot \int_{c_a} e^{-j\frac{k}{2}[G_1(Q_a)\cos^2\theta^i_a](\ell'_1 - \ell'_{1a})^2} d\ell'_1 \\ & + [\hat{R}_b \times \hat{R}_b \times (\hat{n}_b \times \hat{s}^i_b \times \bar{A}(Q_b))] \frac{e^{-jk(s^i_b + s^r_b)}}{\sqrt{s^i_b s^r_b}} \\ & \cdot \int_{c_b} e^{-j\frac{k}{2}[G_1(Q_b)\cos^2\theta^i_b](\ell'_1 - \ell'_{1b})^2} d\ell'_1 \Bigg] \Bigg\} \end{aligned} \tag{13}$$

in which $\bar{A}(Q_{a,b})$ denotes the value of $\bar{A}$ at $Q_{a,b}$; also $G_1(Q_{a,b})$ is defined as

$$G_1(Q_{a,b}) = \frac{1}{s^r_{a,b}} + \frac{1}{\rho^r_{1a,1b}} \text{ , at } Q_{a,b} \, . \tag{14}$$

It can be shown that

$$\frac{1}{\rho^r_{1a,1b}} = \frac{1}{s^i_{a,b}} + \frac{2}{\rho_g(Q_{a,b}) \cos\theta^i_{a,b}} \, . \tag{15}$$

The domains of integration C_a and C_b include the isolated or disjoint neighborhoods of the points Q_a and Q_b on C. The $\rho_g(Q_{a,b})$ denotes the radius of curvature of the boundary C along $\hat{\ell}'_1$ at $Q_{a,b}$; furthermore, $\rho^r_{1a,1b}$ corresponds to the radius of curvature of the reflected wavefront associated with the GO rays reflected from the points $Q_{a,b}$ on C, and $\theta^i_{a,b}$ is the usual angle of incidence (made by the incident ray and the normal to C at $Q_{a,b}$). An evaluation of the integrals over C_a and C_b in (13) after extending the limits of integration to infinity via the stationary phase approach (which yields $\int_{-\infty}^{\infty} e^{-j\frac{k}{2}G\xi^2} d\xi = \left|\sqrt{\frac{2\pi}{kG}}\right| e^{-j\frac{\pi}{4}Sgn(G)}$, wherein $Sgn(G_1(Q_a)) = +1$ and $Sgn(G_1(Q_b)) = -1$ for $G_1(Q_a) > 0$ and $G_1(Q_b) < 0$, respectively.) leads to

$$\begin{aligned}
\bar{E}^s(P_L) \sim \sqrt{\frac{jk}{2\pi}} \Bigg\{ & [\hat{R}_a \times \hat{R}_a \times (\hat{n}_a \times \hat{s}^i_a \times \bar{A}(Q_a))] \frac{e^{-jk(s^i_a + s^r_a)}}{\sqrt{s^i_a s^r_a}} \\
& \cdot \left| \sqrt{\frac{2\pi}{kG_1(Q_a)\cos^2\theta^i_a}} \right| e^{-j\frac{\pi}{4}Sgn(G(Q_a))} \\
& + [\hat{R}_b \times \hat{R}_b \times (\hat{n}_b \times \hat{s}^i_b \times \bar{A}(Q_b))] \frac{e^{-jk(s^i_b + s^r_b)}}{\sqrt{s^i_b s^r_b}} \\
& \cdot \left| \sqrt{\frac{2\pi}{kG_1(Q_b)\cos^2\theta^i_b}} \right| e^{-j\frac{\pi}{4}Sgn(G(Q_b))} \Bigg\} .
\end{aligned} \tag{16}$$

It is noted that

$$\hat{R}_{a,b} \times \hat{R}_{a,b} \times (\hat{n}_{a,b} \times \hat{s}^i_{a,b} \times \bar{A}(Q_{a,b})) = (2\hat{n}_{a,b}\hat{n}_{a,b} - \bar{\bar{I}}) \cdot \bar{A}(Q_{a,b}) \cos\theta^i_{a,b} \tag{17}$$

in which $\bar{\bar{I}}$ is an identity dyad (so that $\bar{\bar{I}} \cdot \bar{A} = \bar{A}$). In two-dimensions, where one is restricted to the $z = 0$ (say) plane; i.e., to the (x,y) plane, then $\bar{\bar{I}} = \hat{x}\hat{x} + \hat{y}\hat{y}$. For example, $\bar{\bar{I}} = \hat{x}\hat{x} + \hat{y}\hat{y} + \hat{z}\hat{z}$ in a rectangular coordinate system. Thus, incorporating (14) and (17) into (16) yields:

$$\bar{E}^s(P_L) \sim \bar{E}^r_a(P_L) + \bar{E}^r_b(P_L) \tag{18}$$

where

$$\bar{E}^r_{a,b}(P_L) \equiv (2\hat{n}_{a,b}\hat{n}_{a,b} - \bar{\bar{I}}) \cdot \bar{A}(Q_{a,b}) \frac{e^{-jks^i_{a,b}}}{\sqrt{s^i_{a,b}}} \cdot \sqrt{\frac{\rho^r_{1a,1b}}{\rho^r_{1a,1b} + s^r_{a,b}}}\, e^{-jks^r_{a,b}}. \tag{19}$$

Since, $\bar{A}(Q_{a,b}) \frac{e^{-jks^i_{a,b}}}{\sqrt{s^i_{a,b}}}$ can be identified as $\bar{E}^i(Q_{a,b})$ (see comments below (3)), the preceeding result becomes:

$$\bar{E}^r_{a,b}(P_L) \equiv \bar{E}^i(Q_{a,b}) \cdot \bar{\bar{R}}(Q_{a,b}) \sqrt{\frac{\rho^r_{1a,1b}}{\rho^r_{1a,1b} + s^r_{a,b}}}\, e^{-jks^r_{a,b}} \tag{20}$$

where

$$\bar{\bar{R}}(Q_{a,b}) \equiv 2\hat{n}_{a,b}\, \hat{n}_{a,b} - \bar{\bar{I}} \tag{21}$$

can be recognized as the dyadic reflection coefficient for a perfectly conducting boundary. Consequently, the non-uniform asymptotic result for $\bar{E}^s(P_L)$ in (18) together with (20) can be identified as the sum of the fields associated with the two GO rays reflected from the points $Q_{a,b}$ as shown in Figures 1(a) and 1(b). It is noted that one must require $G_1(Q_a) > 0$ and $G_1(Q_b) < 0$ to be consistent with

Figures 1(a) and 1(b); thus,

$$\sqrt{\frac{\rho_{1a}^r}{\rho_{1a}^r + s_a^r}} = \left|\sqrt{\frac{\rho_{1a}^r}{\rho_{1a}^r + s_a^r}}\right| \text{ , since } G_1(Q_a) > 0 \text{ ,} \tag{22}$$

and

$$\sqrt{\frac{\rho_{1b}^r}{\rho_{1b}^r + s_b^r}} = \left|\sqrt{\frac{\rho_{1b}^r}{\rho_{1b}^r + s_b^r}}\right| e^{j\frac{\pi}{2}} \text{ , since } G_1(Q_b) < 0 \text{ ,} \tag{23}$$

must be true in (19) and (20) as required by (16). Clearly, (22) and (23) indicate that the principal (positive) branch of the square roots must be taken. As usual, the additional phase $e^{j\frac{\pi}{2}}$ in (23) indicates that the GO ray reflected from the point Q_b touches the caustic before reaching P_L as shown in Figures 1(a) and 1(b). It is convenient to express the reflection coefficient $\overline{\overline{R}}$ in terms of the unit vectors fixed in the incident and reflected rays [16] as shown in Figure 1(c) ; thus,

$$\overline{\overline{R}} = R_s \hat{e}_\perp \hat{e}_\perp + R_h \hat{e}_{||}^i \hat{e}_{||}^r \quad ;$$

$$\underset{h}{R_s} = \mp 1 \text{ for a conducting boundary.} \tag{24}$$

The non-uniform asymptotic high frequency or the GO approximation for the refelcted field $\bar{E}^s(P_L)$ at P_L which is valid on the lit side of the caustic but external to the caustic transition region is given explicitly via (16) through (24) as:

$$\bar{E}^s(P_L) \sim \bar{E}^i(Q_a) \cdot \overline{\overline{R}}(Q_a) \left|\sqrt{\frac{\rho_{1a}^r}{\rho_{1a}^r + s_a^r}}\right| e^{-jks_a^r}$$

$$+ \bar{E}^i(Q_b) \cdot \overline{\overline{R}}(Q_b) \cdot j \left|\sqrt{\frac{\rho_{1b}^r}{\rho_{1b}^r + s_b^r}}\right| e^{-jks_b^r} \text{ .} \tag{25}$$

All the quantities in (25) have been defined previously. It is noted that $\overline{\overline{R}}(Q_{a,b})$ in (25) is as given in (24) except that the unit vectors $\hat{e}_\perp$, $\hat{e}_{||}^i$ and $\hat{e}_{||}^r$ are evaluated

separately for the first and second terms on the right hand side of (25) corresponding to each of the rays reflected from Q_a and Q_b, respectively.

At the caustic $s^r_{\substack{a \\ b}} = \left|\rho^r_{\substack{1a \\ 1b}}\right|$ and $\rho^r_{\substack{1a \\ 1b}} = -\left|\rho^r_{\substack{1a \\ 1b}}\right|$; hence the GO reflected field $\bar{E}^s(P_L)$ in (25) becomes singular there. The representation in (25) is not valid at and near such a caustic of reflected rays.

One can likewise extend the stationary phase analysis into the shadow region; in the latter case, one can show that the scattered field $\bar{E}^S(P_S)$ at a point P_S in the shadow region is given by:

$$\bar{E}^s(P_s) \sim \bar{E}^i(Q^c_b) \cdot \bar{\bar{R}}(Q^a_b)\sqrt{\frac{\rho^{rc}_b}{\rho^{rc}_b + s^{rc}_b}}\; e^{-jks^{rc}_b} \tag{26a}$$

with

$$\bar{E}^i(Q^c_b) = \bar{A}(Q^c_b)\frac{e^{-jks^{ic}_b}}{\sqrt{s^{ic}_b}} \tag{26b}$$

The contribution in (26) is associated with the complex stationary phase point Q^c_b corresponding to $\ell' = \ell'_b$ (see (7)), which must lie on the complex extension of the reflecting boundary as discussed by Ikuno and Felsen [2]; the contribution from the other (conjugate) stationary phase point at Q^c_a corresponding to $\ell' = \ell'_a$ must be discarded on physical grounds since it gives rise to an exponentially increasing field amplitude as mentioned before. The contribution in (25) can be shown to be exponentially decreasing corresponding to an evanescent field at P_S on the dark side of the caustic. The superscript c in the quantities appearing in (26) denotes that those quantities are associated with the "complex" stationary point Q^c_b.

It is noted that the quantity ρ^{rc}_b on the right hand side of (26) is calculated via an analytic continuation of the corresponding expression for ρ^r_b in (15). This follows

because the point of specular reflection Q_b on the actual boundary in real space for an observation point $P = P_L$ on the lit side of the caustic is analytically continued to a complex location Q_b^c, which obviously must lie on the complex extension of the original boundary when $P = P_S$ for an observation point on the dark side of the caustic [1]. Thus, when the right hand side (RHS) of the expression in (15) is evaluated at the real stationary point Q_b, then one obtains the value denoted by ρ_b^r which appears on the left hand side (LHS) of (15); likewise, when the (RHS) of (15) is evaluated at a complex stationary point Q_b^c, then one obtains the analytic continuation of ρ_b^r from its value at the real coordinates of Q_b to its value at the complex coordinates of Q_b^c. The manner in which the quantities s_b^{ic}, s_b^{rc}, $\rho_g(Q_b^c)$, $\cos\theta_b^{ic}$ (= value of $\cos\theta^i$ in (10) evaluated at Q_b^c), ρ_b^{rc}, etc., are evaluated for the complex stationary point Q_b^c by a simple analytic continuation of the corresponding expressions given in (8)-(11) and (15) for real stationary points, is described in the Appendix for the sake of completeness and convenience. Also, the $\overline{\overline{R}}(Q_b^c)$ may be found by analytic continuation of $\overline{\overline{R}}(Q_b)$ in (21) to the complex location Q_b^c in place of Q_b, or by evaluating $\overline{\overline{R}}$ in (24) at Q_b^c; either of these procedures should yield the same result for $\overline{\overline{R}}(Q_b^c)$. If (21) is used, then the $\hat{n}_b$ therein which is evaluated at Q_b must be replaced by $\hat{n}_b^c$ when it is evaluated at Q_b^c; similarly, if one employs (24), then the $\hat{e}_\perp^i$, $\hat{e}_{||}^i$, $\hat{e}_{||}^r$ must be replaced by their analytically continued values $\hat{e}_\perp^c$, $\hat{e}_{||}^{ic}$ and $\hat{e}_{||}^{rc}$ for the complex stationary point Q_b^c as shown in the Appendix. The expression in (26) also becomes singular at the caustic where Q_b^c, ρ_{1b}^{rc}, s_b^{rc}, etc., become real and $\rho_{1b}^{rc} = -\mid \rho_{1b}^{rc} \mid$ as well as $s_b^{rc} = \mid \rho_{1b}^{rc} \mid$; hence, (26) is also not valid at and near the caustic. A uniform representation valid at and near the reflected ray caustic which recovers the results in (25) and (26) for the lit and dark sides of the caustics that

lie outside the caustic transition region is described next.

II-B Uniform 2-D Analysis

The starting point for the analysis is again the integral representation for the scattered field $\bar{E}^s(P)$ which is given in (1). This integral will be evaluated via a uniform asymptotic procedure [6] to overcome the limitations (near the caustic) of the non-uniform solution which was developed in Part A of this section. Again, one may make the usual approximations which lead to (4) as before. The results in (5), (6) and (7) are still valid. However, instead of incorporating the local phase approximation of (12) into (4), which is valid if the stationary points are isolated (or not close together) as it happens when one is outside the caustic transition region, one must now employ a different procedure which remains valid even where the stationary points come close together as it happens for observation points near the caustic. Thus, instead of (12), one employs the following transformation when $P = P_L$ on the lit side of the caustic:

$$s^i + R = \frac{1}{3}\, t^3 - \zeta_\ell\, t + \delta_\ell \quad ; \quad \zeta_\ell > 0 \tag{27}$$

where

$$\delta_\ell = \frac{1}{2}\ [(s_b^i + s_b^r) + (s_a^i + s_a^r)] \tag{28}$$

and

$$\zeta_\ell^{\frac{3}{2}} = \frac{3}{4}\ [(s_b^i + s_b^r) - (s_a^i + s_a^r)]\ . \tag{29}$$

all the quantities on the RHS of (28) and (29) have been defined previously in Part A (also see Figures 1(a) and 1(b)). Substituting (27) into (4) yields

$$\bar{E}^s(P_L) \approx e^{-jk\delta_\ell} \int_{-\infty}^{\infty} dt\ \bar{F}(t)\ e^{-jk(\frac{1}{3}t^3 - \zeta_\ell t)} \tag{30}$$

with

$$\bar{F}(t) \equiv \sqrt{\frac{jk}{2\pi}}\ [\hat{R} \times \hat{R} \times (\hat{n} \times \hat{s}^i \times \bar{A})] \frac{1}{\sqrt{s^i R}}\ \frac{d\ell_1'}{dt}. \tag{31}$$

The limits of integration in (30) have been extended to infinity even if C is a finite closed contour because in the present development one is interested only in the contribution from the saddle points which dominates near the caustic; the contribution from the end points at $\pm\infty$ is vanishingly small. Any other contributions to the radiation integral in (4) which may arise due to a finite closed contour C must be added separately and are not dealt with here.

Following Chester, et al. [6], one may now expand $\bar{F}(t)$ in (31) as

$$\bar{F}(t) = \sum_{m=0}^{\infty} [\bar{a}_m (t^2 - \zeta_\ell)^m + \bar{b}_m t (t^2 - \zeta_\ell)^m] \tag{32}$$

Retaining only the leading term ($m = 0$ term) in the above expansion of (32) yields the following result for $\bar{E}^s(P_L)$ in (30):

$$\bar{E}^s(P_L) \sim 2\pi j\ e^{-jk\zeta_\ell}\ [\bar{P}_\ell k^{-\frac{1}{3}} Ai(-k^{\frac{2}{3}}\zeta_\ell) + j\zeta_\ell^{-\frac{1}{2}} \bar{Q}_\ell k^{-\frac{2}{3}} Ai'(-k^{\frac{2}{3}}\zeta_\ell)] + 0(k^{-1}) \tag{33}$$

in which $Ai(\sigma) = \frac{1}{2\pi} \int_{-\infty}^{\infty} e^{-j(\frac{t^3}{3} + \sigma t)}\ dt$; and $Ai'(\sigma) = \frac{d}{d\sigma} Ai(\sigma)$. It can be shown that the $\bar{P}_L$ and $\bar{Q}_L$ in (33) are given by:

$$\begin{Bmatrix} \bar{P}_\ell \\ \bar{Q}_\ell \end{Bmatrix} = \zeta^{\frac{1}{4}} \sqrt{\frac{k}{\pi}} \begin{bmatrix} \bar{B}_a \cos^2\theta_a^i & e^{-j\frac{\pi}{4}} \\ \sqrt{s_a^i\ s_a^r} & \sqrt{G_1(Q_a)} \cos^2\theta_a^i \end{bmatrix}$$

$$\mp \frac{\bar{B}_b \cos\theta_b^i}{\sqrt{s_b^i\, s_b^i}} \quad \frac{e^{+j\frac{\pi}{4}}}{\sqrt{G_1(Q_b)\cos\theta_b^i}}\Bigg] \quad , \tag{34}$$

with

$$\bar{B}_{a,b}\cos\theta_{a,b}^i \equiv \hat{R}_{a,b} \times \hat{R}_{a,b} \times \left[\hat{n}_{a,b} \times \hat{n}_{a,b} \times \bar{A}(Q_{a,b})\right] \quad . \tag{35}$$

It follows from (17), (19) and (20) that the preceeding result in (35) can be written as

$$\bar{B}_{a,b}\cos\theta_{a,b}^i = \bar{A}(Q_{a,b}) \cdot \bar{\bar{R}}(Q_{a,b})\cos\theta_{a,b}^i \tag{36}$$

in which $\bar{A}(Q_{a,b})$ is given by $\bar{E}^i(Q_{a,b}) = \bar{A}(Q_{a,b})\frac{e^{-jks_{a,b}^i}}{\sqrt{s_{a,b}^i}}$ as indicated previously below (26). Incorporating (37) together with (14) into (34) and (35) gives

$$\left\{ \begin{array}{c} \bar{P}_\ell \\ \bar{Q}_\ell \end{array} \right\} = \zeta_\ell^{\frac{1}{4}} \; 2\sqrt{\frac{k}{\pi}} \left[\frac{\bar{A}(Q_a)\cdot\bar{\bar{R}}(Q_a)}{\sqrt{s_a^i}} \sqrt{\frac{\rho_{1a}^r}{\rho_{1a}^r + s_a^r}}\, e^{-j\frac{\pi}{4}} \right.$$
$$\left. \mp \frac{\bar{A}(Q_b)\cdot\bar{\bar{R}}(Q_b)}{\sqrt{s_b^i}} \sqrt{\frac{\rho_{1b}^r}{\rho_{1b}^r + s_b^r}}\, e^{+j\frac{\pi}{4}} \right] \quad . \tag{37}$$

with the understanding that (22) and (23) are true in (37). It is noted that $\bar{A}(Q_{a,b})$ can depend on $Q_{a,b}$ not only via $\hat{e}_{||}^i$ and $\hat{e}_\perp$ in terms of which the polarization of $\bar{E}^i$ can be expressed, but there could be additional pattern information of the source contained in $\bar{A}$ as a result of which $\bar{A}$ can also depend on $\hat{s}_{a,b}^i$ (that along with $\hat{e}_{||}^i$ and $\hat{e}_\perp$ in turn depends on $Q_{a,b}$). On the lit side exterior to the caustic transition region, the result for $\bar{E}^s(P_L)$ in (33) toegther with (28), (29) and (37), uniformly reduces to the GO result in (25). One can verify this GO limit by employing the asymptotic approximations for $Ai(-k^{\frac{2}{3}}\zeta_\ell)$ and $Ai'(-k^{\frac{2}{3}}\zeta_\ell)$ in (33) for $\zeta_\ell >> 1$ corresponding to

the lit side of the caustic which lies exterior to the caustic transition region; these asymptotic approximations are:

$$Ai(-k^{\frac{2}{3}}\zeta_\ell) \sim \frac{1}{\sqrt{\pi}}\, k^{-\frac{1}{6}}\zeta_\ell^{-\frac{1}{4}} \sin(\frac{2}{3}k\zeta_\ell^{\frac{3}{2}} + \frac{\pi}{4}) \; ; \; \zeta_\ell >> 1 \; , \tag{38}$$

$$Ai'(-k^{\frac{2}{3}}\zeta_\ell) \sim -\frac{1}{\sqrt{\pi}}\, k^{\frac{1}{6}}\zeta_\ell^{\frac{1}{4}} \cos(\frac{2}{3}k\zeta_\ell^{\frac{3}{2}} + \frac{\pi}{4}) \; ; \; \zeta_\ell >> 1 \; . \tag{39}$$

A uniform result similar to that in (33) can also be obtained for the shadow side of the caustic; this uniform analysis for the shadow side is presented next. Once again, the starting point is the integral representation in (4). A transformation similar to that in (27) is introduced into the phase term in the integrand of (4) when $P = P_L$ on the shadow side of the caustic as

$$s^i + R = \frac{1}{3}\, t^3 + \zeta_s t + \delta_s \; ; \; \zeta_s > 0, \tag{40}$$

to account for the proximity of the stationary phase points Q_a^c and Q_b^c in the phase function $(s^i + R)$, which occur on the complex extension of the original boundary (see (7)). Also,

$$\delta_s = \frac{1}{2}\, [(s_b^{ic} + s_b^{rc}) + (s_a^{ic} + s_a^{rc})] \tag{41}$$

and

$$\zeta_s^{\frac{3}{2}} = j\frac{3}{4}\, [(s_b^{ic} + s_b^{rc}) - (s_a^{ic} + s_a^{rc})] \; . \tag{42}$$

The s_b^{ic} and s_b^{rc} in (41) and (42) are the same as those seen previously in (26a; 26b); these quantities are the analytically continued values of s_b^i and s_b^r from those associated originally with the real stationary point Q_b to the complex stationary point

at Q_b^c as shown in the Appendix. Likewise, s_a^{ic} and s_a^{rc} in (41) and (42) represent the analytically continued values of s_a^i and s_a^r from those associated originally with the real stationary point Q_a to the complex stationary point at Q_a^c. Substituting (40) into (4) yields

$$\bar{E}^s(P_S) \approx e^{-jk\delta_s} \int_{-\infty}^{\infty} dt \bar{F}(t) e^{-jk(\frac{1}{3}t^3 + \zeta_s t)} \tag{43}$$

where $\bar{F}(t)$ was defined earlier in (31). Again, one begins by expanding $\bar{F}(t)$ as in (32); next, retaining only the m=0 term in that expansion leads to the following uniform result for the scattered field $\bar{E}^s(P_S)$ valid on the dark side of the caustic:

$$\bar{E}^s(P_S) \sim 2\pi j \; e^{-jk\zeta_s} [\bar{P}_s k^{-\frac{1}{3}} Ai(k^{\frac{2}{3}}\zeta_s) + \zeta_s^{-\frac{1}{2}} \bar{Q}_s k^{-\frac{2}{3}} Ai'(k^{\frac{2}{3}}\zeta_s)] + O(k^{-1}) \tag{44}$$

in which

$$\left\{ \begin{array}{c} \bar{P}_s \\ \bar{Q}_s \end{array} \right\} = \frac{\zeta_s^{\frac{1}{4}} \; e^{j\frac{\pi}{4}}}{2} \sqrt{\frac{k}{\pi}} \left[\frac{\bar{A}(Q_a^c) \cdot \bar{\bar{R}}(Q_a^c)}{\sqrt{s_a^{ic}}} \sqrt{\frac{\rho_{1a}^{rc}}{\rho_{1a}^{rc} + s_a^{rc}}} \; e^{-j\frac{\pi}{4}} \right.$$
$$\left. \mp \frac{\bar{A}(Q_b^c) \cdot \bar{\bar{R}}(Q_b^c)}{\sqrt{s_b^{ic}}} \sqrt{\frac{\rho_{1b}^{rc}}{\rho_{1b}^{rc} + s_b^{rc}}} \; e^{+j\frac{\pi}{4}} \right] \; . \tag{45}$$

It is noted that since ζ_s in (42) is positive (see (40)), the quantity within the square brackets in (42) satisfies the conditions

$$Re[(s_b^{ic} + s_b^{rc}) - (s_a^{ic} + s_a^{rc})] = 0 \; , \tag{46}$$

$$Im[(s_b^{ic} + s_b^{rc} - (s_a^{ic} + s_a^{rc})] > 0 \; .$$

On the shadow side exterior to the caustic transition region, the result for $\bar{E}^s(P_S)$ in (44) together with (41), (42), and (45) reduces uniformly to the analytically continued GO result in (26) for the field reflected from Q_b^c. One can verify this limiting value in (26) for the expression in (44), by employing the asymptotic approximations for $Ai(k^{\frac{2}{3}}\zeta_s)$ and $Ai'(k^{\frac{2}{3}}\zeta_s)$ in (44) for $\zeta_s >> 1$ corresponding to the dark side of the caustic which lies exterior to the caustic transition region; these asymptotic approximations are:

$$Ai(k^{\frac{2}{3}}\zeta_s) \sim \frac{1}{2\sqrt{\pi}}(k^{\frac{2}{3}}\zeta_s)^{-\frac{1}{4}} e^{-(\frac{2}{3}k\zeta_s^{\frac{3}{2}})} \quad ; \quad \zeta_s >> 1 \quad , \tag{47}$$

$$Ai'(k^{\frac{2}{3}}\zeta_s) \sim -\frac{1}{2\sqrt{\pi}}(k^{\frac{2}{3}}\zeta_s)^{\frac{1}{4}} e^{-(\frac{2}{3}k\zeta_s^{\frac{3}{2}})} \quad ; \quad \zeta_s >> 1 \quad . \tag{48}$$

It is important to observe that even though the values associated with both complex stationary points Q_a^c and Q_b^c, respectively, are present in the expressions for $\left\{ \begin{array}{c} \bar{P}_s \\ \bar{Q}_s \end{array} \right\}$ in (45), the use of (47) and (48) in (44) yields an asymptotic limit containing only the field reflected from the complex stationary point Q_b^c (and not Q_b^c).

III An Asymptotic Solution for the Field Associated with a Three-Dimensional Smooth Caustic:

The development presented in Section 2 for the 2-D case is repeated here for the corresponding 3-D situation. The excitation, as in the 2-D case, is assumed to be produced by a localized source such that the field incident on the 3-D reflecting boundary can be represented ray optically. Again, both the non-uniform and the uniform asymptotic approximations of the PO integral for the scattered field in 3-D are presented separately in Parts A and B of this section, respectively. As before, the non-uniform asymptotics yield the pair of GO reflected ray fields on the lit side of the smooth caustics of reflected rays that are associated with the two real stationary points correspond to points of reflection at Q_a and Q_b on the 3-D reflecting boundary. These two reflected GO rays coalesce at the caustic where their non-uniform GO field becomes unbounded. The non-uniform field on the dark side of the caustic is associated with only one of the two complex stationary points which yields an exponentially decaying field behavior (the other does not satisfy the radiation condition); this complex stationary point is denoted by Q_b^c on the complex extension of the reflecting boundary. Once again, it is noted that the non-uniform analysis is not valid at and near the smooth caustics of reflected rays; one must instead employ the results based on the uniform analysis within these caustic regions. The non-uniform result for the dark side of the caustic is also unbounded at the caustic. Of course, the uniform results reduce to the non-uniform results outside

the caustic transition regions. As done for the 2-D case, the non-uniform analysis serves to introduce the notation for the 3-D case which will also be employed in the uniform asymptotic analysis.

In the 3-D case, there can in general be two smooth caustics of reflected rays; the present analysis is valid across each caustic provided that these two caustic surfaces do not intersect. For the sake of convenience of analysis, it is assumed that the 3-D reflecting boundary is rotationally symmetric (about the z-axis (say)), and that the observation point lies in the plane defined by the point source (which illuminates the boundary) and the axis of revolution (or z-axis) of the rotationally symmetric boundary. Under this assumption, the plane of incidence (or reflection) defined by the incident ray direction and the normal to the surface both of which are evaluated at the real point of reflection on the boundary coincides with one of the principal planes of that boundary. While this situation arises only in special cases, it is chosen because it simplifies the analysis. Furthermore the asymptotic results obtained in this special case can be employed directly to deal also with the general case in which the boundaries are not necessarily rotationally symmetric, and in which the planes of incidence do not necessarily coincide with any of the principal planes of the surface at real points of specular reflection on the boundary.

III-A Non-Uniform 3-D Analysis:

The electric field $\bar{E}^s(P)$ which is scattered by a 3-D boundary illuminated by a ray optical field (chosen here to be that due to a point source at P'), and which is observed at a point P exterior to the boundary can be expressed as usual in terms

of the induced current $\bar{J}$ on the boundary S by:

$$\bar{E}^s(P) \approx \frac{jkZ_o}{4\pi}\int_s\int [\hat{R}\times\hat{R}\times\bar{J}(Q'')]\frac{e^{-jkR}}{R}\,ds' \quad , \tag{49}$$

in which Q' is any point on the boundary S and $\bar{R}$ is the vector from Q' to P (or $\bar{R} = \overline{Q'P}$) as before. Also, P cannot be too close to S for (49) to be valid. The PO approximation to (49) is employed via the usual GO approximation $\bar{J}(Q') = 2\hat{n}\times\bar{H}^i(Q')$, (on the lit portion of S and zero otherwise) given in (2), where $\hat{n}$ is the unit outward normal vector to S at Q' and the incident ray optical magnetic field $\bar{H}^i(Q')$ due to a point source at P' is given by

$$\bar{H}^i(Q') \sim Z_o^{-1}\hat{s}^i\times\bar{A}\,\frac{e^{-jks^i}}{s^i} \quad ; \quad \hat{s}^i\cdot\bar{A} = 0 \tag{50}$$

As usual, $\bar{H}^i(Q') \approx Z_o^{-1}\hat{s}^i\times\bar{E}^i(Q')$, in which the incident electric field $\bar{E}^i(Q') = \bar{A}\,\frac{e^{-jks^i}}{s^i}$. It is noted that $\bar{s}^i = P'Q'$ as in the 2-D case, and $s^i = \frac{\bar{s}^i}{|\bar{s}^i|}$.

Since one is primarily interested in the fields specularly reflected from the surface, it will be assumed that the boundaries of the PO integration (resulting from the shadow boundary on the surface) are far from the stationary points in the exponential phase term of the integrand; furthermore, these spurious contributions to the PO integral arising from the shadow boundary will be ignored. For the sake of convenience, the region of integration will still be denoted by S. Thus, under the PO approximation, (49) becomes:

$$\bar{E}^s(P) \approx \frac{jk}{2\pi}\int_s\int \hat{R}\times\hat{R}\times(\hat{n}\times\hat{s}^i\times\bar{A})\frac{e^{-jk(s^i+R)}}{s^iR}\,ds' \tag{51}$$

Let $ds' = d\ell'\cdot d'\ell_2'$, where ℓ_1' is the coordinate curve corresponding to the generator of the 3-D surface of revolution S and ℓ_2' is the azimuthal coordinate which is

orthogonal to ℓ_1'. As in the 2-D case, the phase term $e^{-jk(s^i+R)}$ exhibits real stationary phase points at Q_a and Q_b on S if $P = P_L$ on the lit side of the smooth caustic; likewise it exhibits complex stationary points at Q_a^c and Q_b^c (which are complex conjugates of each other) if $P = P_S$ on the dark side of the caustic. The stationary phase condition is given by:

$$\hat{\ell}_1' \cdot \nabla(s^i + R) = 0 \;\; ; \;\; \hat{\ell}_2' \cdot \nabla(s^i + R) = 0 \;\; . \tag{52}$$

Both the above conditions (namely (52a) and (52b)) must be satisfied simultaneously at the stationary points. If the source point and the axis of revolution of S define the plane $\ell_2' = \ell_{2s}'$, and if the observation point lies in this plane then (52a; 52b) can be shown to yield stationary phase points for which

$$\ell_2' = \ell_{2s}' \;\; \text{(at stationary phase points)} \tag{53}$$

along with $\ell_1' = \ell_{1a}'$ for Q_a and $\ell_1' = \ell_{1b}'$ at Q_b, if $P = P_L$. Thus, the coordinates of Q_a are $(\ell_{1a}'; \ell_{2s}')$ and of Q_b are $(\ell_{1b}'; \ell_{2s}')$, respectively. Likewise, when $P = P_S$, the coordinates of Q_a^c are $(\ell_{1a}^c; \ell_{2s}')$ and of Q_b^c are $(\ell_{1b}^c; \ell_{2s}')$. The quantities $\ell_{1a}', \ell_{1b}', \ell_{1a}^c$ and ℓ_{1b}^c have the same meaning as in (6a; 6b) and (7) for the 2-D case.

At the real stationary points Q_a and Q_b on S for $P = P_L$ the realtionships given in (8)-(11) for the 2-D case also hold for the present 3-D situation because the condition $\ell_2' = \ell_{2s}'$ at the stationary phase points describes a plane which reduces the 3-D problem effectively into a 2-D problem. The reflected rays in Figures 1(a) and 1(b) for the 2-D case also exist in the plane $\ell_2' = \ell_{2s}'$ for the 3-D case except that the boundary in those figures must be modified to become rotationally symmetric for the present 3-D analysis.

In the neighborhood of the stationary points Q_a and Q_b when $P = P_L$, one may employ the following local approximation for the phase term $k(s^i + R)$:

$$s^i + R \approx s^i_{a,b} + s^r_{a,b} + \frac{1}{2} G_1(Q_{a,b}) \cos^2 \theta^i_{a,b} (\ell'_1 - \ell'_{1a,1b})^2 + \frac{1}{2} G_2(Q_{a,b})(\ell'_2 - \ell'_{2s})^2 \ , \quad \text{for } Q' \text{ near } Q_{a,b} \ . \tag{54}$$

At high frequencies (or large k), the dominant contribution to (51) comes from the stationary phase points Q_a and Q_b on S when $P = P_L$; therefore, (51) is approximated via (54) to obtain:

$$\bar{E}^s(P_L) \approx \frac{jk}{2\pi} \left[e^{-jk(s^i_a + s^r_a)} \int_{s_1} \int d\ell'_1 d\ell'_2 \left\{ [\hat{R} \times \hat{R} \times (\hat{n} \times \hat{s}^i \times \bar{A}(Q'))] \cdot \frac{1}{s^i R} \cdot e^{-j\frac{k}{2} G_1(Q_a)(\ell'_1 - \ell'_{1a})^2} \ e^{-j\frac{k}{2} G_2(Q_a)(\ell'_2 - \ell'_{2s})^2} \right\} \right.$$
$$\left. + e^{-jk(s^i_b + s^r_b)} \int_{s_2} \int d\ell'_1 \, d\ell'_2 \ \left\{ [\hat{R} \times \hat{R} \times (\hat{n} \times \hat{s}^i \times \bar{A}(Q'))] \frac{1}{s^i R} \cdot e^{-j\frac{k}{2} G_1(Q_b)(\ell'_1 - \ell'_{1b})^2} \ e^{-j\frac{k}{2} G_2(Q_b)(\ell'_2 - \ell'_{2s})^2} \right\} \right] \tag{55}$$

in which $G_1(Q_{a,b})$ is given as before in (14) together with (15). Likewise, $G_2(Q_{a,b})$ is defined as:

$$G_2(Q_{a,b}) = \frac{1}{s^r_{a,b}} + \frac{1}{\rho^r_{2a,2b}} \quad , \quad \text{at } Q_{a,b} \ . \tag{56}$$

It can be shown that

$$\frac{1}{\rho^r_{2a,2b}} = \frac{1}{s^i_{a,b}} + \frac{2 \cos \theta^i_{a,b}}{\rho_t(Q_{a,b})} \ . \tag{57}$$

The domains of integration s_1 and s_2 in (55) include the disjoint neighborhoods of the points Q_a and Q_b on S. In (57), $\rho_t(Q_{a,b})$ denotes the radius of curvature of S along $\hat{\ell}'_2$ at $Q_{a,b}$; whereas $\rho_g(Q_{a,b})$ which occurs in (14) via (15) is the radius of

curvature of S along $\hat{\ell}_1'$ at $Q_{a,b}$ as indicated previously. Additional approximations valid near Q_a and Q_b in the integrals over s_1 and s_2 of (55) yield

$$\begin{aligned}\bar{E}^s(P_L) \approx \frac{jk}{2\pi}\Bigg\{&[\hat{R}_a \times \hat{R}_a \times (\hat{n}_a \times \hat{s}_a^i \times \bar{A}(Q_a))]\frac{e^{-jk(s_a^i+s_a^r)}}{s_a^i s_a^r} \\ &\cdot \int_{-\infty}^{\infty} d\ell_2'\, e^{-j\frac{k}{2}G_2(Q_a)(\ell_2'-\ell_{2_s}')^2} \cdot \int_{-\infty}^{\infty} d\ell_1'\, e^{-j\frac{k}{2}G_1(Q_a)\cos^2\theta_a^i(\ell_1'-\ell_{1_a}')^2} \\ &+[\hat{R}_b \times \hat{R}_b \times (\hat{n}_b \times \hat{s}_b^i \times \bar{A}(Q_b))]\frac{e^{-jk(s_b^i+s_b^r)}}{s_b^i s_b^r} \\ &\cdot \int_{-\infty}^{\infty} d\ell_2'\, e^{-j\frac{k}{2}G_2(Q_b)(\ell_2'-\ell_{2_b}')^2} \cdot \int_{-\infty}^{\infty} d\ell_1'\, e^{-j\frac{k}{2}G_1(Q_b)\cos^2\theta_a^i(\ell_1'-\ell_1')^2}\Bigg\} \quad (58)\end{aligned}$$

Following essentially the same steps which lead one from (15) to (16) for the 2-D case, it can be easily seen that (56) reduces in the non-uniform stationary phase evaluation to:

$$\begin{aligned}\bar{E}^s(P_L) \approx \frac{jk}{2\pi}\Bigg\{&[\hat{R}_a \times \hat{R}_a \times (\hat{n}_a \times \hat{s}_a^i \times \bar{A}(Q_a))]\frac{e^{-jk(s_a^i+s_a^r)}}{s_a^i s_a^r} \\ &\cdot \left|\sqrt{\frac{2\pi}{kG_1(Q_a)\cos^2\theta_a^i}}\right| e^{-j\frac{\pi}{4}Sgn[G_1(Q_a)]} \cdot \left|\sqrt{\frac{2\pi}{kG_2(Q_a)}}\right| e^{-j\frac{\pi}{4}Sgn[G_2(Q_a)]} \\ &+[\hat{R}_b \times \hat{R}_b \times (\hat{n}_b \times \hat{s}_b^i \times \bar{A}(Q_b))]\frac{e^{-jk(s_b^i+s_b^r)}}{s_b^i s_b^r} \\ &\cdot \left|\sqrt{\frac{2\pi}{kG_1(Q_b)\cos^2\theta_b^i}}\right| e^{-j\frac{\pi}{4}Sgn[G_1(Q_b)]} \cdot \left|\sqrt{\frac{2\pi}{kG_2(Q_b)}}\right| e^{-j\frac{\pi}{4}Sgn[G_2(Q_b)]}\Bigg\} \quad (59)\end{aligned}$$

Making use of the previously mentioned relationships in (14), (17), (21), (24) and (56) simplifies (59) to the more familiar GO reflected field from as:

$$\begin{aligned}\bar{E}^s(P_L) \sim \bar{E}^i(Q_a)\cdot\bar{\bar{R}}(Q_a)\sqrt{\frac{\rho_{1a}^r}{\rho_{1a}^r+s_a^r}}\sqrt{\frac{\rho_{2a}^r}{\rho_{2a}^r+s_a^r}}e^{-jks_a^r} \\ +\bar{E}^i(Q_b)\cdot\bar{\bar{R}}(Q_b)\sqrt{\frac{\rho_{1b}^r}{\rho_{1b}^r+s_b^r}}\sqrt{\frac{\rho_{2b}^r}{\rho_{2b}^r+s_b^r}}e^{-jks_b^r} \quad (60)\end{aligned}$$

It is noted that $\bar{E}^s(P_L)$ in (60) is the sum of the GO fields reflected from the points Q_a and Q_b on S to P_L on the lit side of the caustic defined by $s_b^r = |\rho_{1b}^r|$ where $\rho_{1b}^r = -|\rho_{1b}^r|$. Also, the relationships in (22) and (23) are true in the result of (60); furthermore,

$$\sqrt{\frac{\rho_{2a,2b}^r}{\rho_{2a,2b}^r + s_{a,b}^r}} = \left|\sqrt{\frac{\rho_{2a,2b}^r}{\rho_{2a,2b}^r + s_{a,b}^r}}\right| \quad , \tag{61}$$

if S is a surface of revolution because $\rho_{2a,2b}^r > 0$, and $G_2(Q_{a,b}) > 0$ in that case since the axis of revolution is now the other caustic of the reflected rays (i.e., the second caustic surface degenerates to a line).

The result in (60) fails at and near the caustics of reflected rays. Although (60) has been developed for the special case of a surface of revolution with the observation point P_L being located in the plane defined by the source point and the axis of revolution, it is also valid for the GO reflection of an arbitrary ray optical field from an arbitrary surface, except that $\rho_{1a,1b}^r$ and $\rho_{2a,2b}^r$ in (60) can no longer be obtained from the simple expressions in (15) and (57), respectively, but instead they must now be obtained from the more complicated expressions in [16,17,18] for the latter more general situation.

A similar stationary phase analysis at a point $P = P_S$ on the shadow side of the caustic defined by $s_b^r = |\rho_{1b}^r|$ with $\rho_{1b}^r = -|\rho_{1b}^r|$ yields the following expression for the scattered field $\bar{E}^s(P_S)$:

$$\bar{E}^s(P_S) \sim \bar{E}^i(Q_b^c)\sqrt{\frac{\rho_{1b}^{rc}}{\rho_{1b}^{rc} + s_b^{rc}}}\sqrt{\frac{\rho_{2b}^{rc}}{\rho_{2b}^{rc} + s_b^{rc}}}\, e^{-jks_b^{rc}} \tag{62a}$$

where,

$$\bar{E}^i(Q_b^c) \sim \bar{A}(Q_b^c)\frac{e^{-jks_b^i}}{s_b^i} \quad . \tag{62b}$$

The expressions in (62a; 62b) are analogous to those in (26a; 26b) for the 2-D case. As mentioned earlier, the field in (62a) is specularly reflected from the point Q_b^c which lies on the complex extension of the original boundary; the contribution from the other (complex conjugate) stationary phase point at Q_a^c must again be discarded on physical grounds as it violates the radiation condition. The contribution in (62a) exhibits an exponentially decaying field at P_S. As in the 2-D case, all the quantities associated with the superscript c must be evaluated via an analytic continuation procedure. The non-uniform stationary phase approximation in (62a) is not valid at the caustic associated with ρ_{1b}^r ; it is unbounded there. A uniform asymptotic approximation which remains valid at and near this caustic is presented below.

III-B Uniform 3-D Analysis

One begins the uniform asymptotic analysis by noting that the non-uniform results in (60) and (62), which become unbounded at $s_b^r = |\rho_{1b}^r|$ with $\rho_{1b}^r = -|\rho_{1b}^r|$, are also valid for the reflection of an arbitrary ray optical incident field from an arbitrary 3-D surface. Furthermore, the only difference between the non-uniform results in (60) and (62), for the 3-D case and the corresponding results in (25) and (26) for the 2-D case are the additional reflected ray divergence factors $\sqrt{\frac{\rho_{2a,2b}^r}{\rho_{2a,2b}^r + s_{a,b}^r}}$ and $\sqrt{\frac{\rho_{2b}^{rc}}{\rho_{2b}^{rc} + s_b^{rc}}}$ which are present in (60) and (62) respectively for the 3-D case. The 3-D case reduces to the 2-D case when $\rho_{2a,2b}^r \to \infty$ and $|\rho_{2b}^{rc}| \to \infty$ so that the spreading of the reflected rays is now restricted only to one plane for the 2-D case, and the other spreading (or ray divergence) factors alluded to above (containing $\rho_{2a,2b}^r$ and ρ_{2b}^{rc}) become unity for the 2-D case. Consequently, the uniform GO result for the 3-D case which reduces to (60) and (62) on the lit and dark sides, respectively, outside

the caustic transition regions can be obtained directly from (33) and (44) together with (37) and (45), respectively, by conjecturing that for the lit side, $\bar{E}^s(P_L)$ is given by

$$\bar{E}^s(P_L) \sim 2\pi\ e^{-jk\delta_\ell}[\bar{P}_\ell\ k^{-\frac{1}{3}} Ai(-k^{\frac{2}{3}}\zeta_\ell) + j\zeta_\ell^{-\frac{1}{2}}\bar{Q}_\ell\ k^{-\frac{2}{3}} Ai'(-k^{\frac{2}{3}}\zeta_\ell)] \tag{63}$$

with δ_ℓ and ζ_ℓ (where $\zeta_\ell > 0$) being the same as in (28) and (29). Also, $\bar{P}_\ell$ and $\bar{Q}_\ell$ are given by a simple modification of (37) to include the additional incident and reflected ray spatial spreading (or divergence) factors; thus,

$$\left\{ \begin{array}{c} \bar{P}_\ell \\ \bar{Q}_\ell \end{array} \right\} = \frac{\zeta_\ell^{\frac{1}{4}}}{2}\sqrt{\frac{k}{\pi}}\left[\frac{\bar{A}(Q_a)\cdot\bar{\bar{R}}(Q_a)}{s_a^i}\sqrt{\frac{\rho_{1a}^r}{\rho_{1a}^r+s_a^r}}\sqrt{\frac{\rho_{2a}^r}{\rho_{2a}^r+s_a^r}}\ e^{-j\frac{\pi}{4}} \right.$$
$$\left. \mp \frac{\bar{A}(Q_b)\cdot\bar{\bar{R}}(Q_b)}{s_b^i}\sqrt{\frac{\rho_{1b}^r}{\rho_{1b}^r+s_b^r}}\sqrt{\frac{\rho_{2b}^r}{\rho_{2b}^r+s_b^r}}\ e^{+j\frac{\pi}{4}} \right] . \tag{64}$$

Likewise, $\bar{E}^s(P_S)$ for the shadow side is given by

$$\bar{E}^s(P_S) \sim 2\pi j\ e^{-j\ k\delta_s}[\bar{P}_s k^{-\frac{1}{3}} Ai(k^{\frac{2}{3}}\zeta_s) + \zeta_s^{-\frac{1}{2}}\bar{Q}_s\ k^{-\frac{2}{3}}\ Ai'(-k^{\frac{2}{3}}\zeta_s)] \tag{65}$$

with δ_s and ζ_s (where $\zeta_s > 0$) being the same as in (41) and (42). In addition, the $\bar{P}_s$ and $\bar{Q}_s$ are given by

$$\left\{ \begin{array}{c} \bar{P}_s \\ \bar{Q}_s \end{array} \right\} = \frac{\zeta_s^{\frac{1}{4}}\ e^{j\frac{1}{4}}}{2}\sqrt{\frac{k}{\pi}}\left[\frac{\bar{A}(Q_a^c)\cdot\bar{\bar{R}}(Q_a^c)}{s_b^{ic}}\sqrt{\frac{\rho_{1a}^{rc}}{\rho_{1a}^{rc}+s_a^{rc}}}\sqrt{\frac{\rho_{2a}^{rc}}{\rho_{2a}^{rc}+s_a^{rc}}}\ e^{-j\frac{\pi}{4}} \right.$$
$$\left. \mp \frac{\bar{A}(Q_b^c)\cdot\bar{\bar{R}}(Q_b^c)}{s_b^{ic}}\sqrt{\frac{\rho_{1b}^{rc}}{\rho_{1b}^{rc}+s_b^{rc}}}\sqrt{\frac{\rho_{2b}^{rc}}{\rho_{2b}^{rc}+s_b^{rc}}}\ e^{+j\frac{\pi}{4}} \right] . \tag{66}$$

Thus, the $\bar{P}_{L,S}$ and $\bar{Q}_{LS}$ above in (64) and (66) are obtained by simply including the transverse ray divergence factors $\frac{1}{\sqrt{s_{a,b}^i}}\sqrt{\frac{\rho_{2a,2b}^r}{\rho_{2a,2b}^r+s_{a,b}^r}}$ and $\frac{1}{\sqrt{s_{a,b}^{ic}}}\sqrt{\frac{\rho_{2a,2b}^{rc}}{\rho_{2a,2b}^{rc}+s_{a,b}^{rc}}}$ into the 2-D results given in (37) and (45); here $\frac{1}{\sqrt{s_{a,b}^i}}$ is the additional transverse spreading

or divergence factor for the incident field associated with a point source, whereas $\sqrt{\frac{\rho^r_{2a,2b}}{\rho^r_{2a,2b}+s^r_{a,b}}}$ is the additional spreading factor for the reflected ray in the 3-D case. The results in (63) and (65) are also valid for the general 3-D case as are the non-uniform results in (60) and (62), with the understanding that $(\rho^r_{1a,1b};\rho^r_{2a,2b})$ and $(\rho^{rc}_{1a,1b};\rho^{rc}_{2a,2b})$ must be found from the more general expressions in [16,17,18] that are valid even when the plane of incidence does not coincide with any of the principal planes of the surface at the point of reflection. Furthermore, the illumination (or the incident field) may be an arbitrary ray optical field (rather than a special point source type illumination). For the point source or spherical wave illumination, $\bar{E}^i(Q')\frac{e^{-jks^i(Q')}}{s^i(Q')}$; thus, for the arbitrary ray optical incident field, the terms $\frac{A(Q')}{s^i(Q')}$ in (64) and (66) must be replaced by $\bar{E}^i_{ARB}(Q')\ e^{+jks^i_{ARB}(Q')}$ where $\bar{E}^i_{ARB}(Q')$ is the incident ray optical field whose phase at Q' is given by $\exp(-jks^i_{ARB}(Q'))$. It is easily verified that the results in (63) and (65) which are valid at the caustic defined by $s^r_b = |\rho^r_{1b}|$ with $\rho^r_{1b} = -|\rho^r_{1b}|$ reduce uniformly to the results in (60) and (62), respectively, outside the caustic transition regions where $\zeta_l >> 1$ and $\zeta_s >> 1$; these limits leading to (60) and (62) can be obtained via the asymptotic approximations for the Airy functions described previously in (38;39) and (47;48).

The uniform results conjectured in (63;64) for $P = P_L$ could be justified by starting with the PO integral for $\bar{E}^s(P)$ in (51) by introducing a local approximation analogous to (27) for the phase term $e^{-jk(s^i+R)}$ in the integrand of (51) which unlike (54) is valid even when Q_a and Q_b are close together; namely

$$s^i + R \approx \frac{1}{3}\, t^3(\ell'_1) - \zeta_\ell\, t(\ell'_1) + \zeta_\ell + \frac{1}{2}\, G_2(t(\ell'_1))(\ell'_2 - \ell'_{2s})^2 \qquad (67)$$

with δ_ℓ and ζ_ℓ as in (28) and (29) for the special case when the observation point at

$P = P_L$ lies in the plane defined by the source point and the axis of revolution as was assumed in the previous non-uniform stationary phase analysis for (51) which led to (60). The $G_2(t(\ell_1'))$ is evaluated at $\ell_2' = \ell_{2_s}'$ and has the general form as in (56); namely

$$G_2(t(\ell_1')) = \frac{1}{s^r(\ell_1')} + \frac{1}{\rho_2^r(\ell_1')} \tag{68}$$

with $s^r(\ell_{1a,1b}') \equiv s_{a,b}^r$ and $\rho_2^r(\ell_{1a,1b}') \equiv \rho_{2a,2b}^r$, in which $(\ell_{1a}', \ell_{2_s}')$ and ℓ_{1b}', ℓ_{2_s}' are the coordinates of the stationary phase points Q_a and Q_b on the line $\ell_2' = \ell_{2_s}'$ as indicated below (53). Incorporating (67) into (51) yields:

$$\bar{E}^s(P) \approx e^{-jk\delta_\ell} \int_{-\infty}^{\infty} dt\ e^{-jk(\frac{1}{3}t^3 - \zeta_\ell t)}$$
$$\cdot \int_{-\infty}^{\infty} d\ell_2' \bar{G}(t, \ell_2') \sqrt{\frac{jk}{2\pi}}\ e^{-j\frac{k}{2}G_2(t)(\ell_2' - \ell_{2_s}')^2} \tag{69}$$

with

$$\bar{G}(t, \ell_2') \equiv \sqrt{\frac{jk}{2\pi}}\ [\hat{R} \times \hat{R} \times (\hat{n} \times \hat{s}^i \times \bar{A}(t, \ell_2')]\ \frac{1}{s^i R}\ \frac{d\ell_1'}{dt} \tag{70}$$

where $t = t(\ell_1')$ as noted earlier. Also, the region of integration has been extended to infinity via the usual stationary phase arguments. Evaluating the inner integral over ℓ_2' first using the stationary phase approximation yields

$$\bar{E}^s(P) \sim e^{jk\delta_\ell} \int_{-\infty}^{\infty} dt\ \left\{ \frac{\bar{G}(t, \ell_{2_s}')}{\sqrt{G_2'(t)}} \right\}\ e^{-jk(\frac{1}{3}t^3 - \zeta_\ell t)}. \tag{71}$$

In obtaining (71), the quantity $\bar{G}(t, \ell_2'\ )$ in (69) is approximated by its value at the stationary point $\ell_2' = \ell_{2_s}'$ when evaluating the inner integral on ℓ_2' in (69). The remaining integral in (71) on $t(\ell_2')$ can be evaluated exactly as in (30)-(33) for the

2-D case to obtain the form of the solution which is the same as in (63) with $\bar{P}_\ell$ and $\bar{Q}_\ell$ given by

$$\left\{ \begin{array}{c} \bar{P}_\ell \\ \bar{Q}_\ell \end{array} \right\} = \frac{\zeta_\ell^{\frac{1}{4}}}{2}\sqrt{\frac{k}{\pi}}\Big[\frac{\bar{A}(Q_a)\cdot\bar{\bar{R}}(Q_a)\cos\theta_a^i}{s_a^i s_a^r}\frac{e^{-j\frac{\pi}{4}}}{\sqrt{G_1(Q_a)\cos_a^i}\sqrt{G_2(Q_a)}} \mp \frac{\bar{A}(Q_b)\cdot\bar{\bar{R}}(Q_b)\cos\theta_b^i}{s_b^i s_b^r}\frac{e^{+j\frac{\pi}{4}}}{\sqrt{G_1(Q_b)\cos_b^i}\sqrt{G_2(Q_b)}}\Big] \qquad (72)$$

in which $G_1^{-1}(Q_{a,b}) = \frac{\rho^r_{1a,1b}s^r_{a,b}}{\rho^r_{1a,1b}+s^r_{a,b}}$, and $G_2^{-1}(Q_{a,b})$ is the same as $G_1^{-1}(Q_{a,b})$ with the subscript 1 replaced by 2. It is then easily verified in the special case of a surface revolution, with P_L being located in the plane containing the axis of revolution of the surface and the source point, that (72) is indeed identical to the one conjectured in (64) using physical arguments.

The result conjectured in (65;66) for the dark side of a caustic can also be justified similarly for the special case of the surface of revolution when P_S is located in the plane containing the axis of revolution and the source point. For the latter case, the δ_ℓ and $-\zeta_\ell$ in (67) must be replaced by δ_s and $+\zeta_s$ where $\zeta_s > 0$, with δ_s and ζ_s is as defined in (41) and (42), respectively.

IV Numerical Results

The 2-D uniform asymptotic solution given in (33) and (37) has been applied here to study the backscattering from boundaries which contain points of inflection. One such application is shown in Figure 2 where a closed concave-convex shaped geometry with an edge is illuminated by a plane wave, and it is of interest to find the far zone backscattered field. In addition to the field of the rays specularly

reflected from this boundary, the edge diffracted ray field is also included in this backsca+ter calculation; however, the effect of the rays that creep around the convex portion of the surface after being excited directly at grazing incidence or by edge diffraction is ignored in this work. Also neglected are the effects connected with the launching of whispering gallery type modes on the concave boundary by the mechanism of edge diffraction, and their subsequent transformation into creeping wave or surface ray modes on the convex position of the boundary past the inflection point. The latter effects which have been ignored may not be negligible far from the reflected ray caustic transition region; hence, the backscattered field has been calculated using the uniform GO results of (33) and (37) together with the singly edge diffracted contribution only for $20° < \theta < 80°$ in Figures 3 and 4 for the case when the incident electric field is perpendicular (i.e., soft case) and parallel (i.e., hard case) to the plane of incidence, respectively. Also shown in Figures 3 and 4 are comparisons with an independent moment method (MM) based calculation; the good agreement between the uniform solution and the corresponding MM solution serves to confirm the accuracy of the uniform solution on both the lit and the dark side of the caustic of reflected rays. It is important to note that the maximum in the backscattered pattern occurs near $\theta = 50°$ which is just on the lit side of the caustic of reflected rays. Thus, the effect of the ray caustic is quite significant in producing a strong backscatter around this aspect angle of $\theta = 50°$. It is further noted that the region corresponding to $\theta < 50°$ is on the dark side of the caustic.

Additional calculations via the present uniform GO analysis have been performed for the far zone backscattering by a 2-D smoothly indented cavity of Figure 5, which is illuminated by an electromagnetic plane wave. The results of these cal-

culations are presented in Figures 7-11. Actually there are three parts to Figures 7-9; in part (a) of these figures the result for the backscattering from the geometry of Figure 5 are presented, whereas, in parts (b) and (c) of each of these figures the backscattering from a 2-D rectangular cavity of the same length and depth are presented for the sake of comparison [19]. The 2-D rectangular cavity geometry is shown in Figure 6. The results in parts (b) and (c) of Figures 7-9 for the backscattering by a rectangular cavity pertain to the cases when the incident electric field is parallel and perpendicular to the plane of incidence, respectively. The results in part (a) of Figures 7-9 are the same for both of these types of incident field polarization over the range of aspects $|\theta| < 60°$ which have been considered. The latter is true because the polarization sensitive creeping or surface ray modes launched on the convex portion of the reflecting boundary outside the smoothly indented cavity portion do not contribute in the range $|\theta| < 60°$, and because the uniform GO reflection contribution from the smooth indentation gives the same dB magnitude levels for the two different incident polarizations (only the phase of the total uniform GO field differs by a sign for the two types of incident polarization). Figures 7-9 pertain to cavities of the same length; only the cavity depth changes in each of these figures. Figures 10 and 11 show the change in the backscattering from the smoothly indented cavity of Figure 5 due to changing the cavity length while keeping the cavity depth fixed. It is seen from Figures 7-11 that the perturbation in the backscattering due to the presence of a cavity is limited to a smaller range of aspects for the smoothly indented cavity as compared to that for the sharp edged rectangular cavity. This is to be expected because the effect of the smoothly indented cavity is significant only within the two reflected ray caustic transition

regions. Nevertheless, it is also observed that the backscattering by the smoothly indented cavities can be approximately of the same order as the rectangular cavity for aspects that lie between the reflected ray caustics. It is noted that there are two reflected ray caustics in the far zone for the problem in Figure 5 (there is one caustic associated with each of the two points of inflection on the smooth cavity). These caustics are non-intersecting in the far zone; however, they can intersect to form higher order caustics in the near zone. The present uniform GO analysis can be employed to find the scattering from the smoothly indented cavity of Figure 5 only for cavity lengths which are large enough so that the two points of inflection and their associated reflected ray caustic transition regions do not come close together. Finally, the present PO based uniform analysis also cannot be used near grazing angles of incidence on the reflecting boundaries with points of inflection. It is proposed as a part of future effort to remove the latter restriction. In conclusion, the present uniform GO solution is shown to be accurate and relatively simple to use within its domain of validity; the conditions under which the uniform GO results remain valid are essentially no different than the conditions required for the conventional GO analysis to be valid.

Appendix

The Parameters Used in the Uniform GO Calculation

In this appendix, one defines the parameters which have been used in the uniform GO solution for the lit side of the caustic. These parameters are then analytically continued to complex coordinate space in order to calculate the field on the shadow side of the caustic. These parameters are presented for the general 3-D case; however one can easily obtain the 2-D results by requiring $z = 0$ in the 3-D results.

Parameters for the Lit Side of the Caustic

Let the coordinates of the source point P' and the observation point P_L be denoted by (x', y', z') and (x_L, y_L, z_L), respectively. For the sake of being specific, one may choose the real point of reflection Q_b on the actual reflecting boundary; let the coordinates of this point Q_b on the surface be (x_b, y_b, z_b). Then one can define the ray path lengths s_b^i, s_b^r, the direction of the incident ray $\hat{s}_b^i$, the direction of the reflected ray $\hat{s}_b^r$, the surface normal $\hat{n}_b$ at Q_b, the scalar product between the surface normal and the reflected ray direction $\cos\theta_b^i$, the radius of curvature of the surface ρ_g at Q_b and the vectors $\hat{e}_\perp$, $\hat{e}_{\|}^i$, and $\hat{e}_{\|}^r$ associated with the incident and reflected ray for the point of Q_b as the following:

$$s_b^i = \sqrt{(x_b - x')^2 + (y_b - y')^2 + (z_b - z')^2} \tag{73}$$

$$s_b^r = \sqrt{(x_L - x_b)^2 + (y_L - y_b)^2 + (z_L - z_b)^2} \tag{74}$$

$$\hat{s}_b^i = \frac{1}{s_b^i}\left[(x_b - x')\hat{x} + (y_b - y')\hat{y} + (z_b - z')\hat{z}\right] \tag{75}$$

$$\hat{s}_b^r = \frac{1}{s_b^r}\left[(x_L - x_b)\hat{x} + (y_L - y_b)\hat{y} + (z_L - z_b)\hat{z}\right] \tag{76}$$

$$\cos(2\theta_b^i) = -\hat{s}_b^i \cdot \hat{s}_b^r \tag{77}$$

$$\cos\theta_b^i = \sqrt{\frac{\cos(2\theta_b^i) + 1}{2}} \tag{78}$$

$$\hat{n}_b = \frac{\hat{s}_b^r - \hat{s}_b^i}{2\cos\theta_b^i} \tag{79}$$

$$\left.\begin{aligned} \hat{e}_\perp &= \tfrac{\hat{s}_b^i \times \hat{s}_b^r}{|\hat{s}_b^i \times \hat{s}_b^r|} \\ \hat{e}_{\|}^i &= \hat{e}_\perp \times \hat{s}_b^i \\ \hat{e}_{\|}^r &= \hat{e}_\perp \times \hat{s}_b^r \\ \rho_g(Q_b) &= \rho_g(x_b, y_b, z_b) \end{aligned}\right\} \tag{80}$$

Parameters for the Shadow Side of the Caustic

When the observation point is on the shadow side of the caustic the point of reflection is no longer real (as is Q_b); it is now replaced by a complex point of reflection Q_b^c as discussed in Sections II and III of the report. The corresponding parameters for the shadow side are denoted by the same symbols as in (74)-(81) for the lit side except that they now contain a superscript c to denote the fact that they are associated with the complex point Q_b^c. Let the coordinates of the observation point P_S on the dark side be (x_s, y_s, z_s). Let the coordinate of the complex reflection point Q_b^c on the complex (or analytically continued part) of the extended surface be (x_b^c, y_b^c, z_b^c). One can then redefine the above parameters for the lit side so that they will be valid for the shadow side by simply replacing the coordinates of Q_b by

those of Q_b^c. Thus, one arrives at the following results:

$$s_b^{ic} = \sqrt{(x_b^c - x')^2 + (y_b^c - y')^2 + (z_b^c - z')^2} \tag{81}$$

$$s_b^{rc} = \sqrt{(x_L - x_b^c)^2 + (y_L - y_b^c)^2 + (z_L - z_b^c)^2} \tag{82}$$

$$\hat{s}_b^{ic} = \frac{1}{s_b^{ic}}\left[(x_b^c - x')\hat{x} + (y_b^c - y')\hat{y} + (z_b^c - z')\hat{z}\right] \tag{83}$$

$$\hat{s}_b^{rc} = \frac{1}{s_b^{rc}}\left[(x_L - x_b^c)\hat{x} + (y_L - y_b^c)\hat{y} + (z_L - z_b^c)\hat{z}\right] \tag{84}$$

$$\cos(2\theta_b^{ic}) = -\hat{s}_b^{ic} \cdot \hat{s}_b^{rc} \tag{85}$$

$$\cos\theta_b^{ic} = \sqrt{\frac{\cos(2\theta_b^{ic}) + 1}{2}} \tag{86}$$

$$\hat{n}_b^c = \frac{\hat{s}_b^{rc} - \hat{s}_b^{ic}}{2\cos\theta_b^{ic}} \tag{87}$$

$$\left.\begin{aligned} \hat{e}_\perp^c &= \frac{\hat{s}_b^{ic} \times \hat{s}_b^{rc}}{|\hat{s}_b^{ic} \times \hat{s}_b^{rc}|} \\ \hat{e}_\parallel^{ic} &= \hat{e}_\perp^c \times \hat{s}_b^{ic} \\ \hat{e}_\parallel^{rc} &= \hat{e}_\perp^c \times \hat{s}_b^{rc} \\ \rho_g(Q_b^c) &= \rho_g(x_b^c, y_b^c, z_b^c) \end{aligned}\right\} \tag{88}$$

References

[1] H. Ikuno and L. B. Felsen, "Real and complex rays for scattering from a target with inflection points," Radio Science, Vol. 22, No. 6, pp. 952-958, November 1987.

[2] M. H. Rahnavard and W. V. T. Rusch, "Surface-Curvature-Induced Microwave Shadows," IEEE Transactions on Antennas and Propagation, Vol. AP-30, No.1, pp. 83-88, January 1982.

[3] N. C. Albertsen, P. Balling and N. E. Jensen, "Caustics and Caustic Corrections to the Field Diffracted by a Curved Edge", IEEE Transactions on Antennas and Propagation, Vol. AP-35, No.3, pp. 297-303, May 1977.

[4] Y. A. Kravtsov, "A Modification of the Geometrical Opticas Method," Radiofisica, 7, pp. 664-673, 1964.

[5] D. Ludwig, "Uniform Asymptotic Expansion at a Caustic," Communication on Pure and Applied Mathematics, Vol. XIX, pp. 215-250, 1966.

[6] C. Chester, B. Friedman and F. Ursell, "An Extension of the Method of Steepest Descent," Proceeding of Cambridge Philosophical Society, Vol. 54, pp. 599-611, 1957.

[7] L. B. Felsen and N. Marcuvitz, Radiation and Scattering of Waves, Prentice-Hall, 1973.

[8] J. J. Stamnes, Waves in Focal Region, Adam Hilger (Bristol & Boston), 1986.

[9] I. Kay and J. B. Keller, "Asymptotic Evaluation of the Field at a Caustic," Journal of Applied Physics, Vol. 25, No. 7, pp 876-883, July 1954.

[10] R. N. Buchal and J. B. Keller, "Boundary Layer Problems in Diffraction Theory," Communication on Pure and Applied Mathematics, Vol. XIII, pp. 85-114, 1960.

[11] V. P. Maslov, "Perturbation Theory and Asymptotic Method," Dounod, Paris, 1972. (in French)

[12] R. W. Ziolkowski and G. A. Deschamps, "Asymptotic Evaluation of High Frequency Fields Near a Caustic: an Introduction to Maslov's Method," Radio Science, Vol. 17, pp. 1181-1191, 1984.

[13] M. V. Berry and C. Upstill, "Catastrophe Optics: Morphologies of Caustics and their Diffraction Patterns", Chpater IV in Progress in Optics XVIII, Ed. E. Wolf, North-Holland, 1980.

[14] J. M. Arnold, "Spectral Synthesis of Uniform Wavefunctions,"Wave Motion, No. 8, pp. 135-150, 1986.

[15] J. M. Arnold, "Geometrical Theories of Wave Propagation : A Contemporary Review," IEE Proceedings, Vol. 133, Pt. J, No. 2, pp. 165-188, April, 1986.

[16] G. A. Deschamps, "Ray Techniques in Electromagnetics," Proceedings IEEE, Vol. 60, pp. 1022-1035, September 1972.

[17] R. G. Kouyoumjian and P. H. Pathak, "A Uniform Geometrical Theory of Diffraction for an Wedge in a Perfectly Conducting Surface," Proceedings

IEEE, Vol. 62, pp. 1448-1461, November 1974.

[18] P. H. Pathak, W. D. Burnside and R. J. Marhefka, "A Uniform GTD Analysis of the Diffraction of Electromagnetic Waves by a Smooth Convex Surface," IEEE Transactions on Antennas and Propagation, Vol. AP-28, No. 5, pp. 631-642, September 1980.

[19] M. C. Liang, P. H. Pathak and C. W. Chuang, "An Efficient Hybrid GTD-Modal Analysis of the Scattering by an Open-ended Dielectric Filled Cavity in a Ground Plane," The Ohio State University ElectroScience Lab., Dept. Elec. Eng., Technique Report 716611-2, 1987.

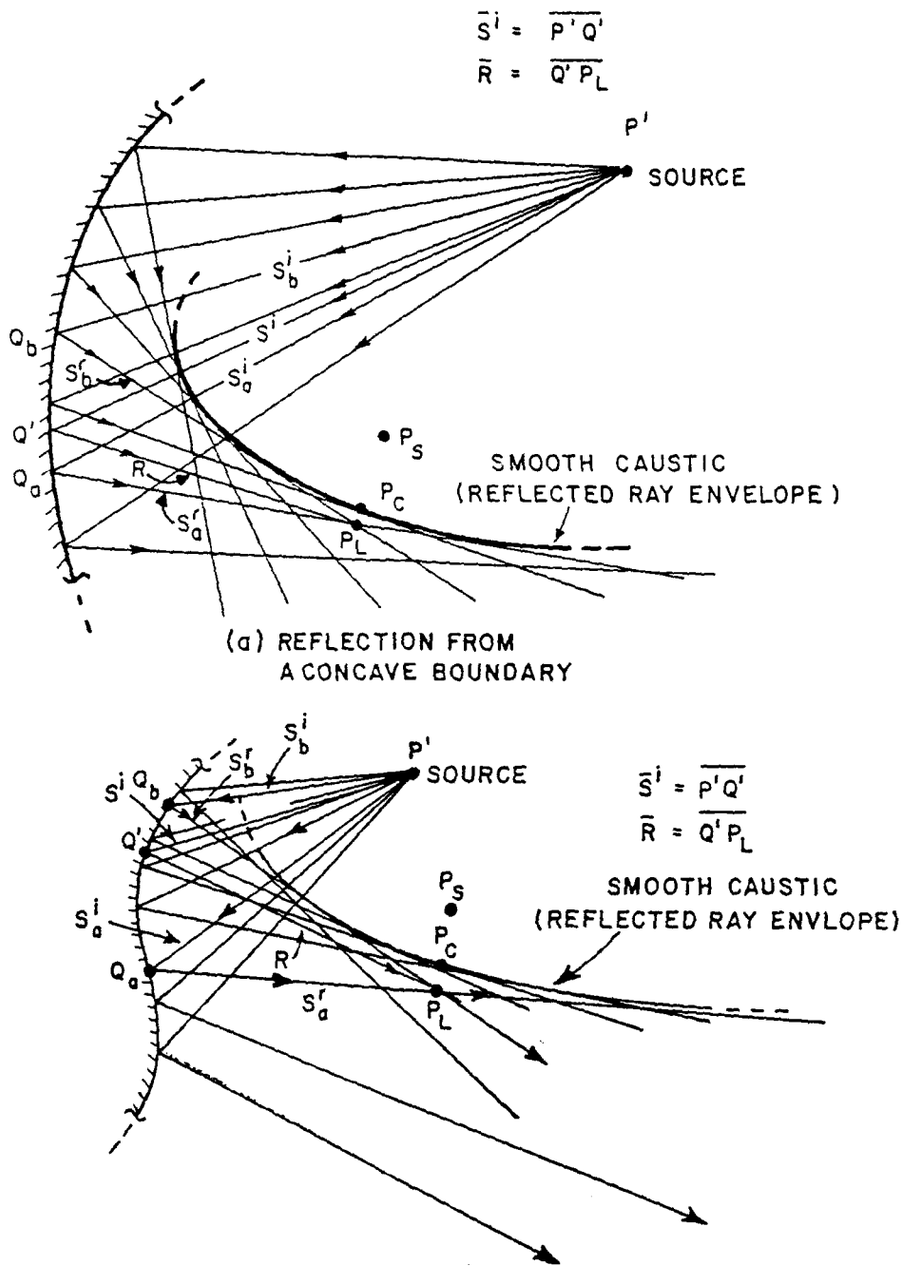

Figure 1: Scattering by smooth boundaries which produce smooth caustics of reflected rays.

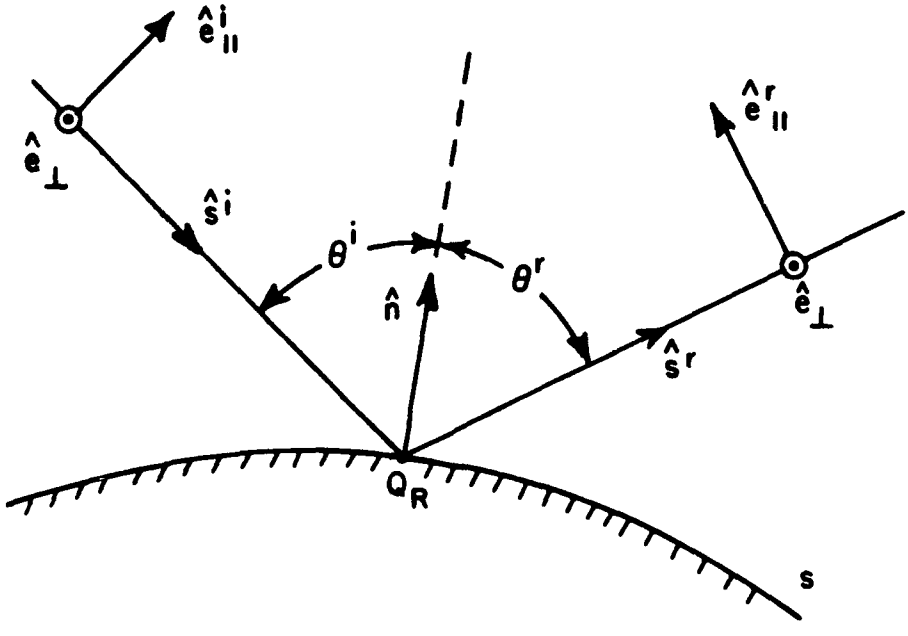

(c)

Figure 1: (continued)

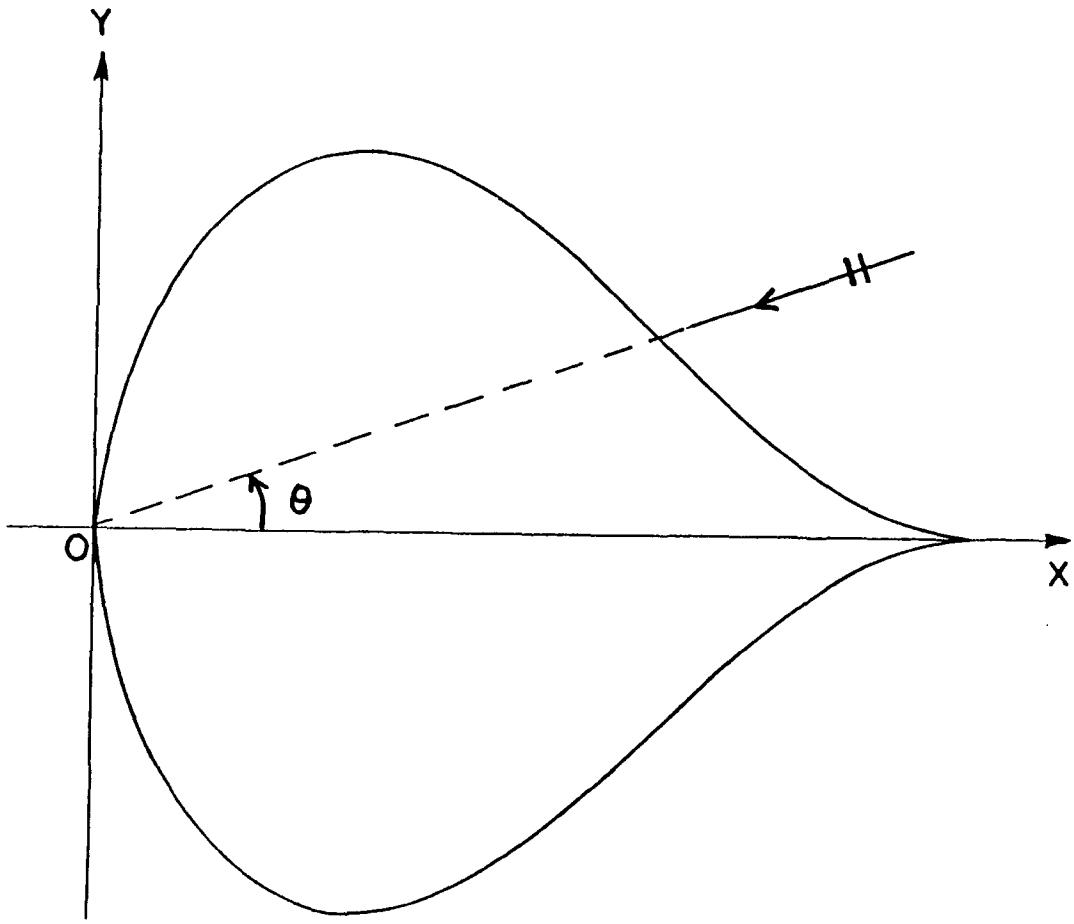

The boundary is defined by the equation

$$y = \frac{1}{2} A \sqrt{\frac{x}{A}} (\cos(\frac{\pi x}{A} + 1)$$

with $A = 0.3\, m$ being the maximum length in the $\hat{x}$ direction

and the frequency at which the calculations of backscatter are made is 3 GHz.

Figure 2: Scattering by a boundary with a point of inflection.

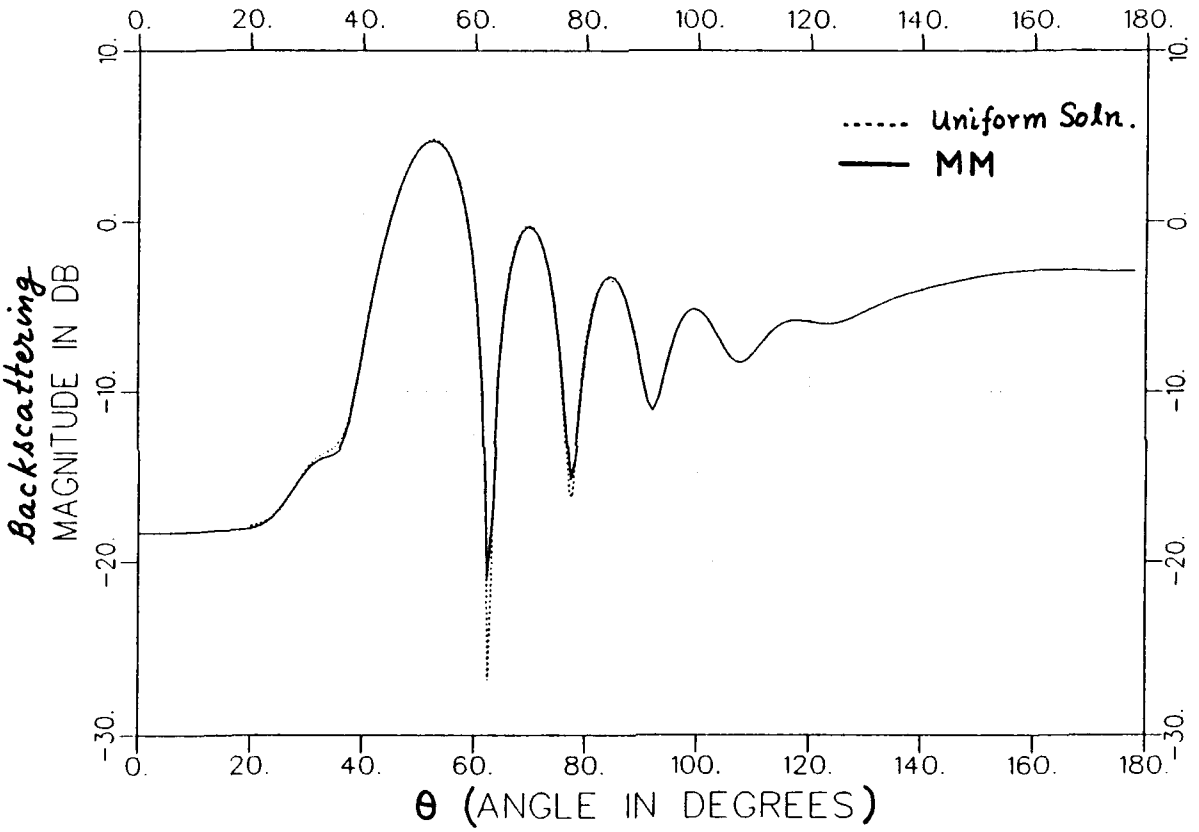

Figure 3: Backscattering from the geometry in Figure 2 when the electric field is polarized perpendicular to the plane of incidence.

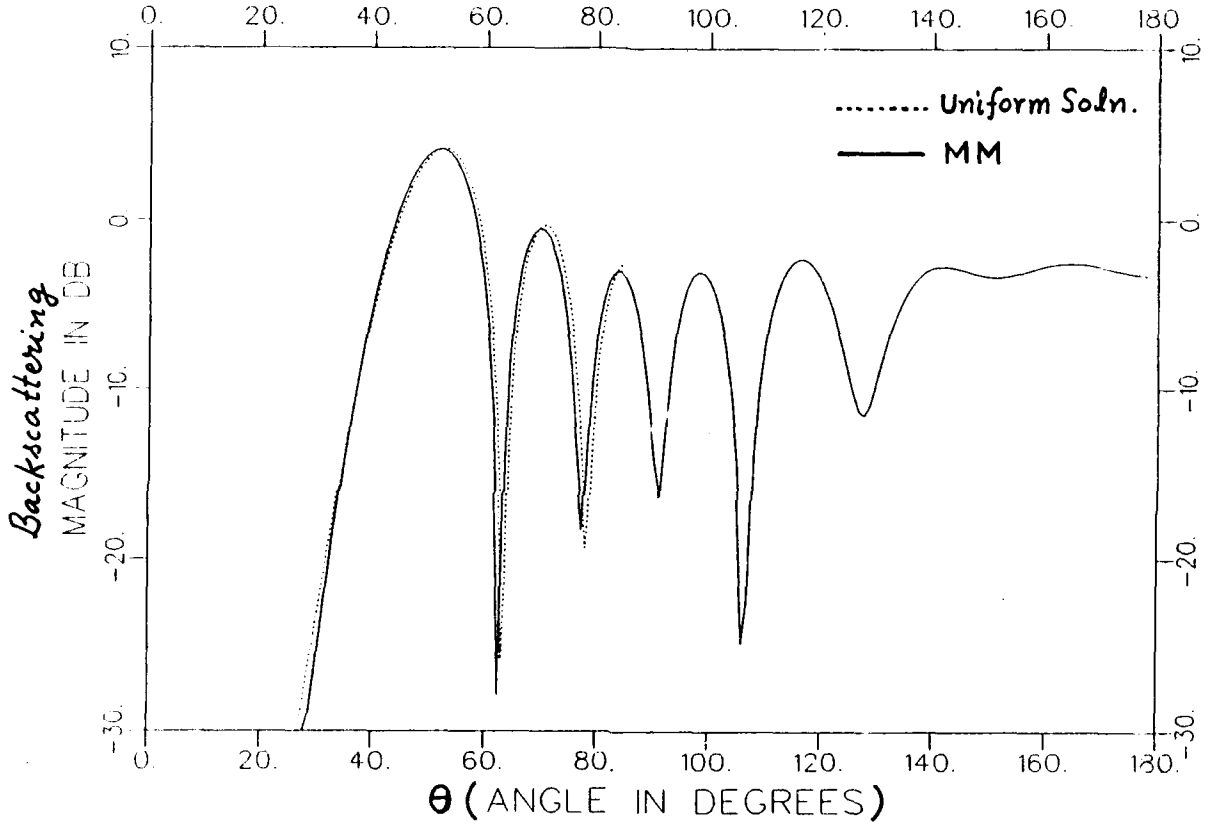

Figure 4: Backscattering from the geometry in Figure 2 when the electric field is polarized parallel to the plane of incidence.

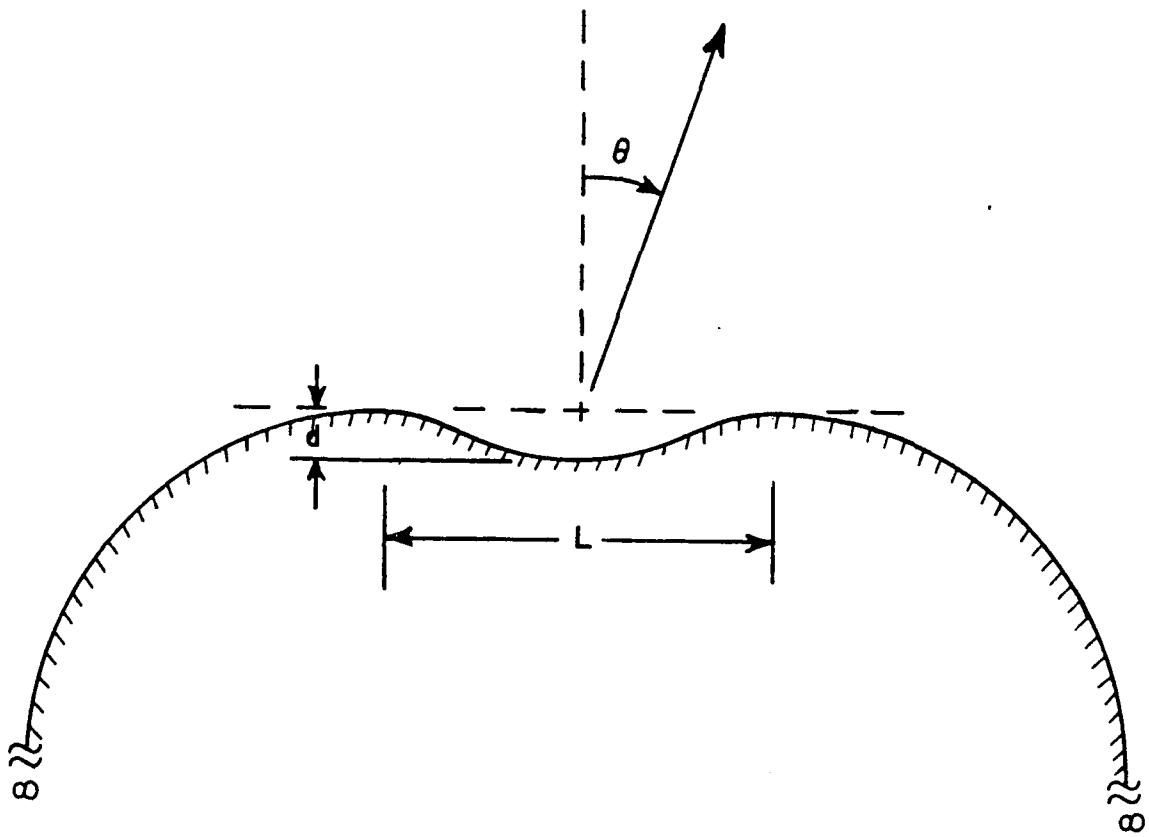

Figure 5: Smoothly indented cavity configuration.

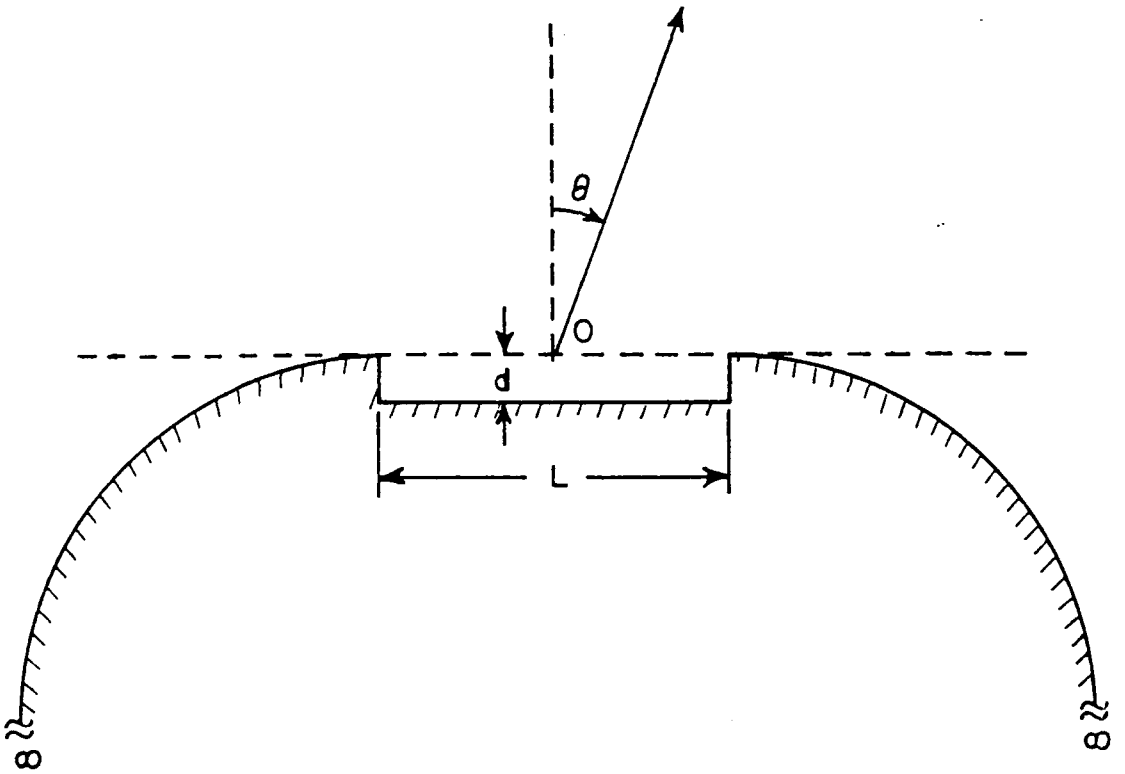

Figure 6: Rectangular cavity configuration.

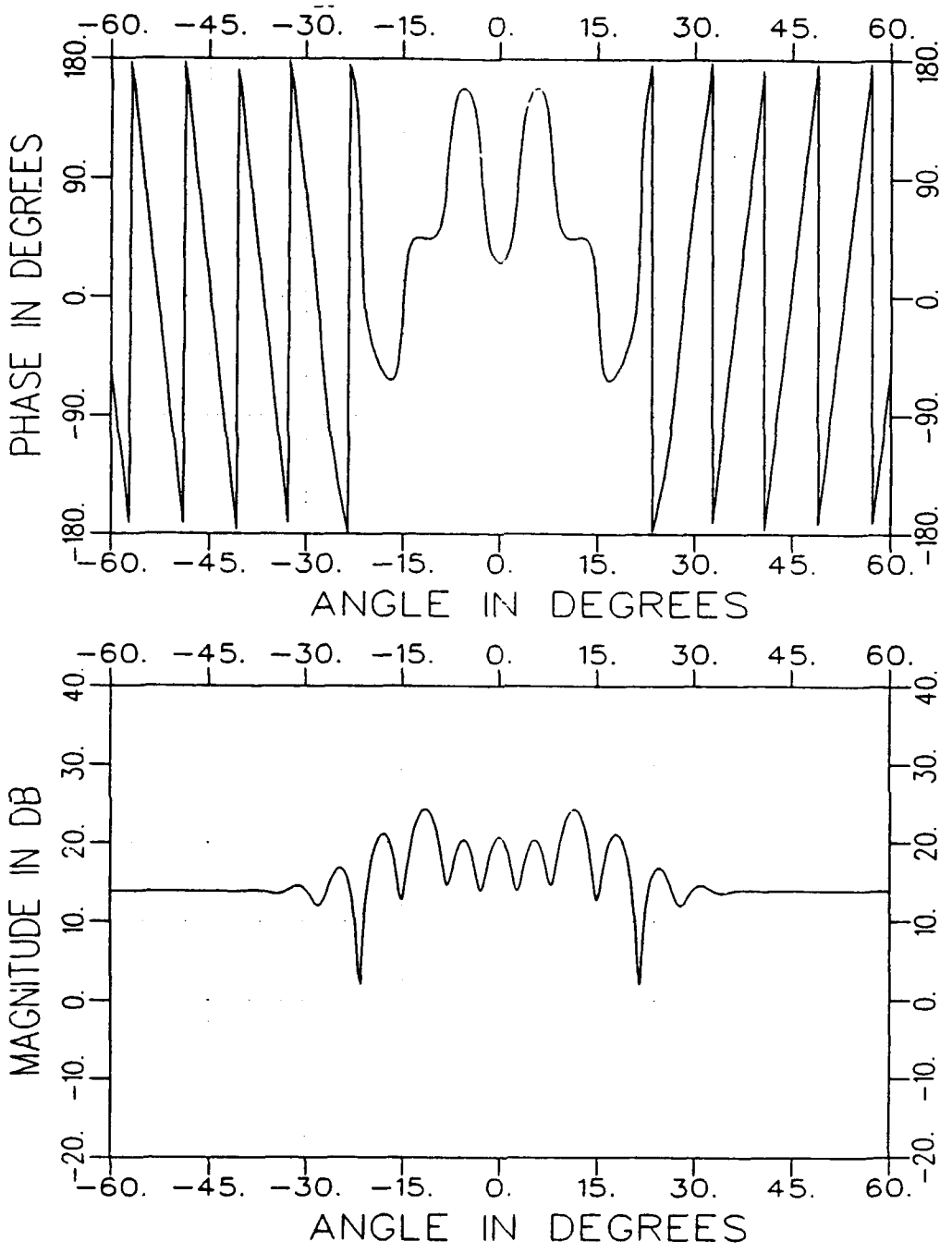

(a) Backscattering by a smoothly indented cavity (Figure 5) of $L = 10.2\lambda$ and $D = 1.\lambda$.

Figure 7: Backscattering by a smoothly indented cavity (of Figure 5) as well as by a rectangular cavity (of Figure 6).

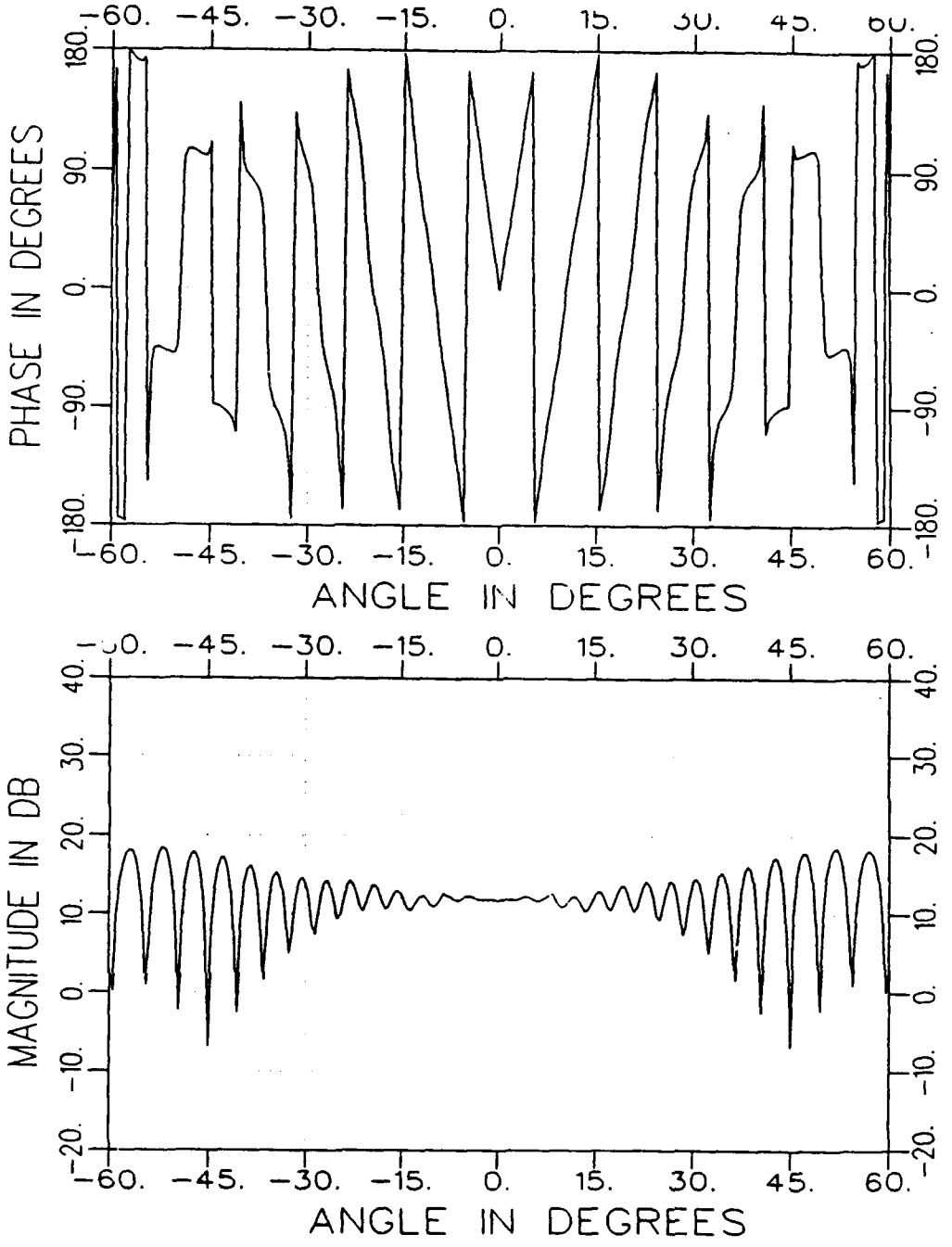

(b) Backscattering by a rectangular cavity (Figure 6) of $L = 10.2\lambda$ and $D = 1.\lambda$ when the electric field is parallel to the plane of incidence.

Figure 7: (continued)

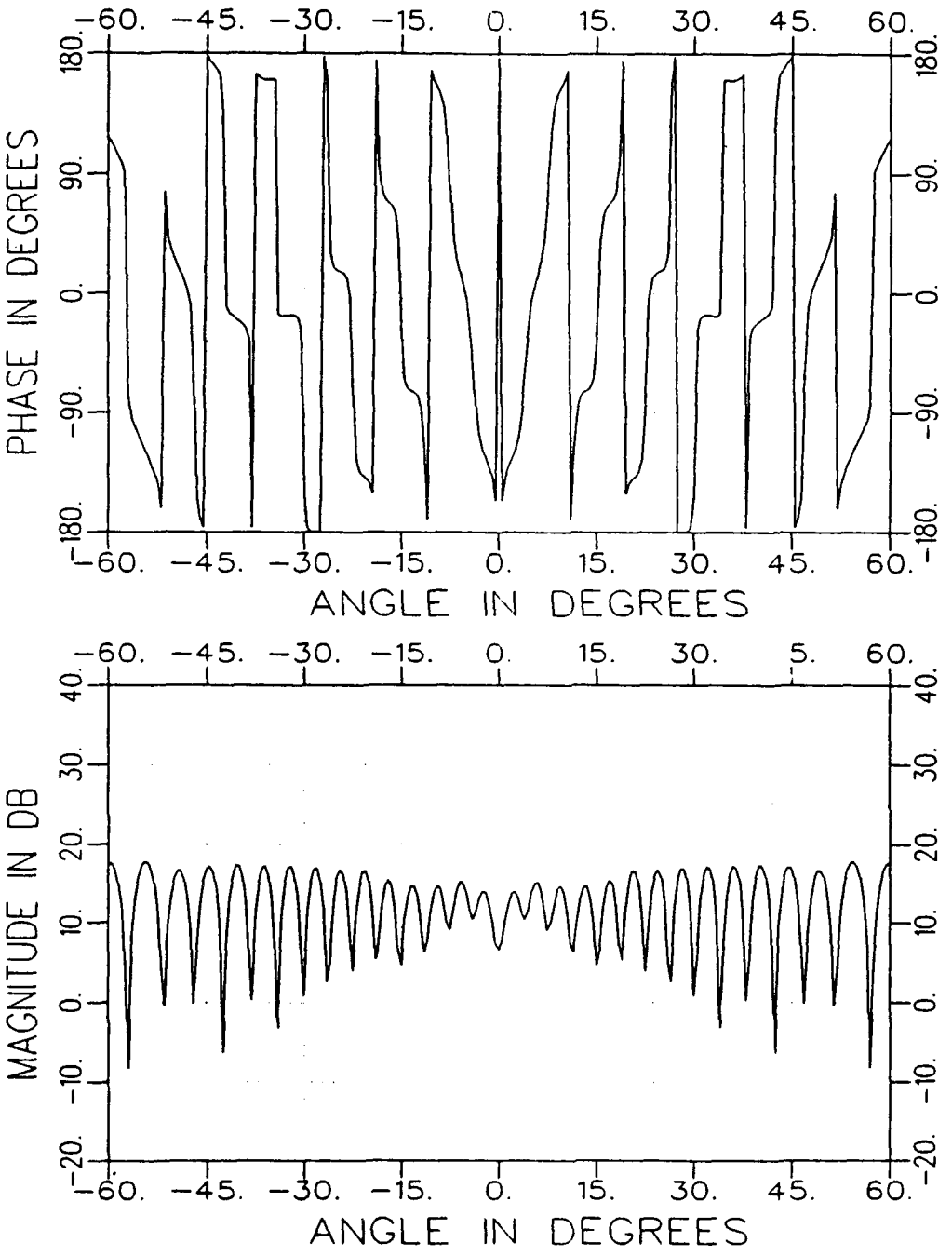

(c) Backscattering by a rectangular cavity (Figure 6) of $L = 10.2\lambda$ and $D = 1.\lambda$ when the electric field is perpendicular to the plane of incidence.

Figure 7: (continued)

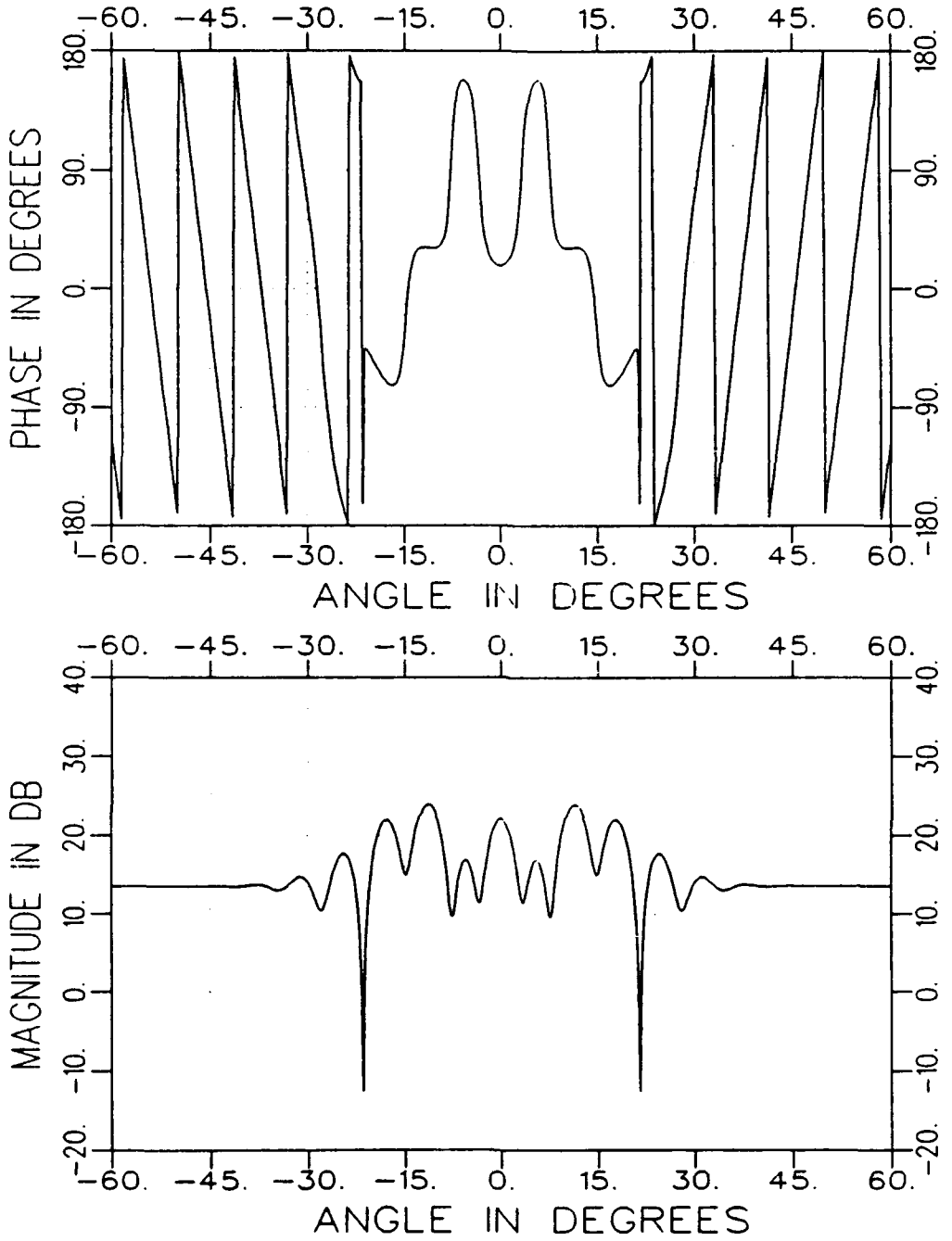

(a) Backscattering by a smoothly indented cavity (Figure 5) of $L = 10.2\lambda$ and $D = 1.1\lambda$.

Figure 8: Backscattering by a smoothly indented cavity (of Figure 5) as well as by a rectangular cavity (of Figure 6).

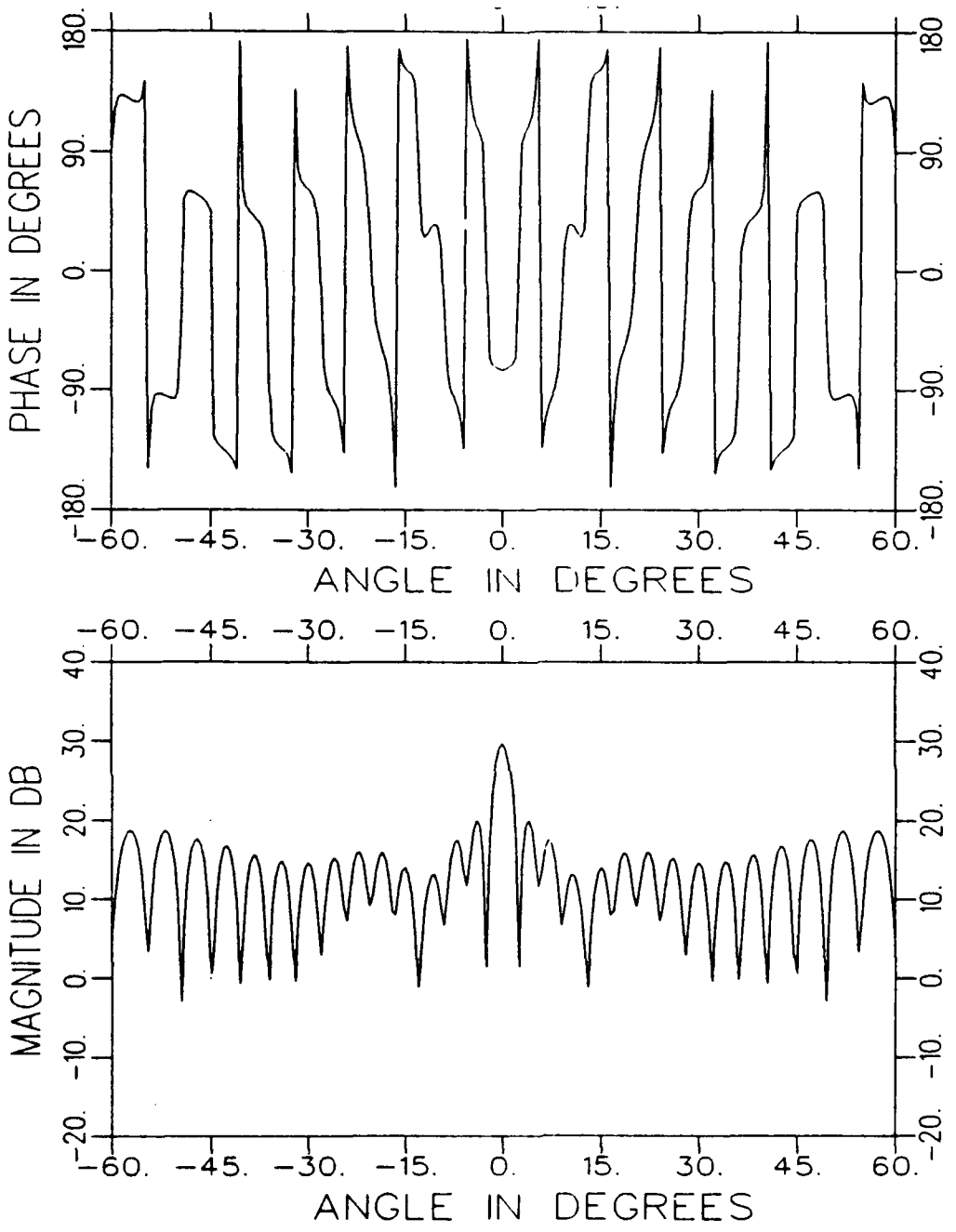

(b) Backscattering by a rectangular cavity (Figure 6) of $L = 10.2\lambda$ and $D = 1.1\lambda$ when the electric field is parallel to the plane of incidence.

Figure 8: (continued)

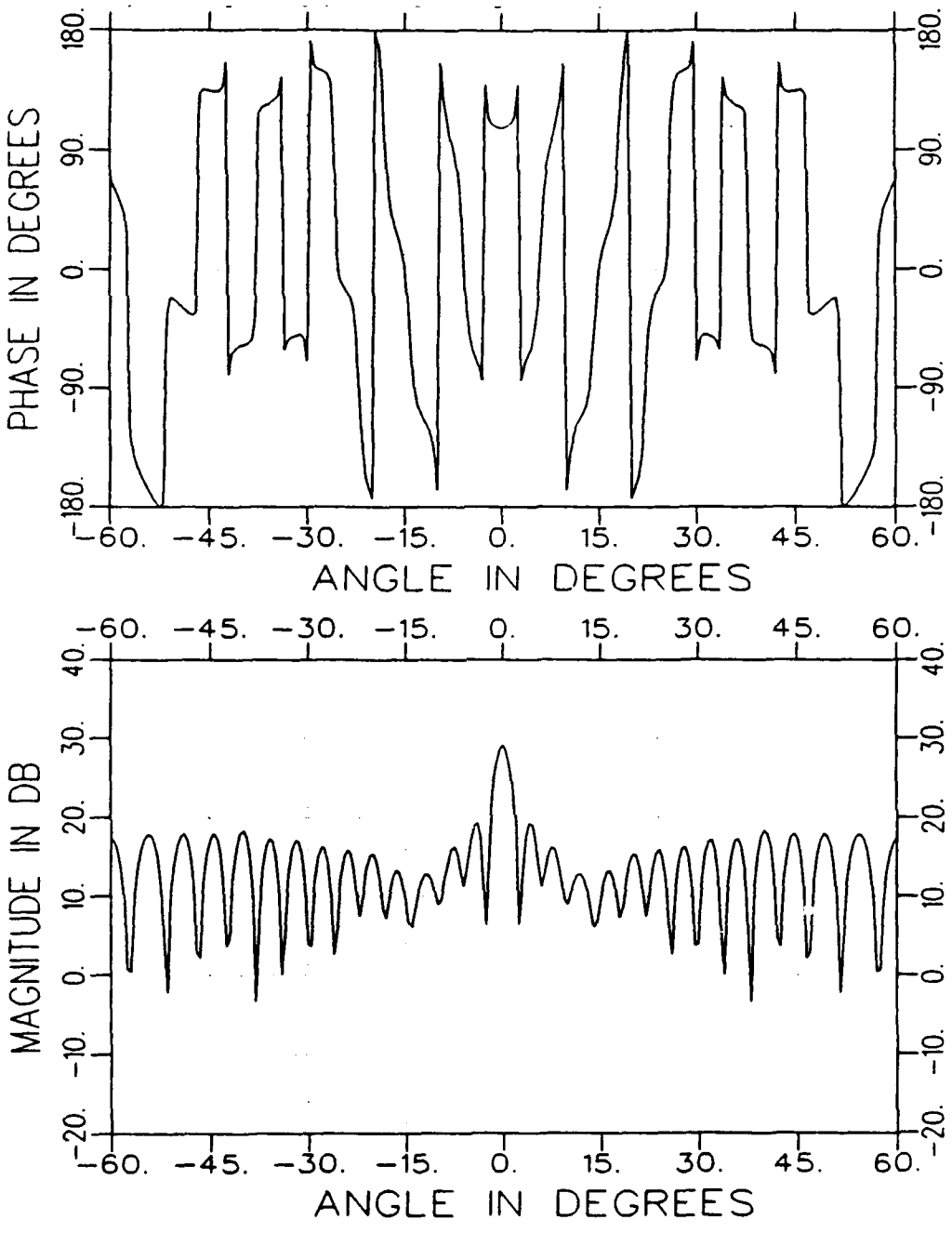

(c) Backscattering by a rectangular cavity (Figure 6) of $L = 10.2\lambda$ and $D = 1.1\lambda$ when the electric field is perpendicular to the plane of incidence.

Figure 8: (continued)

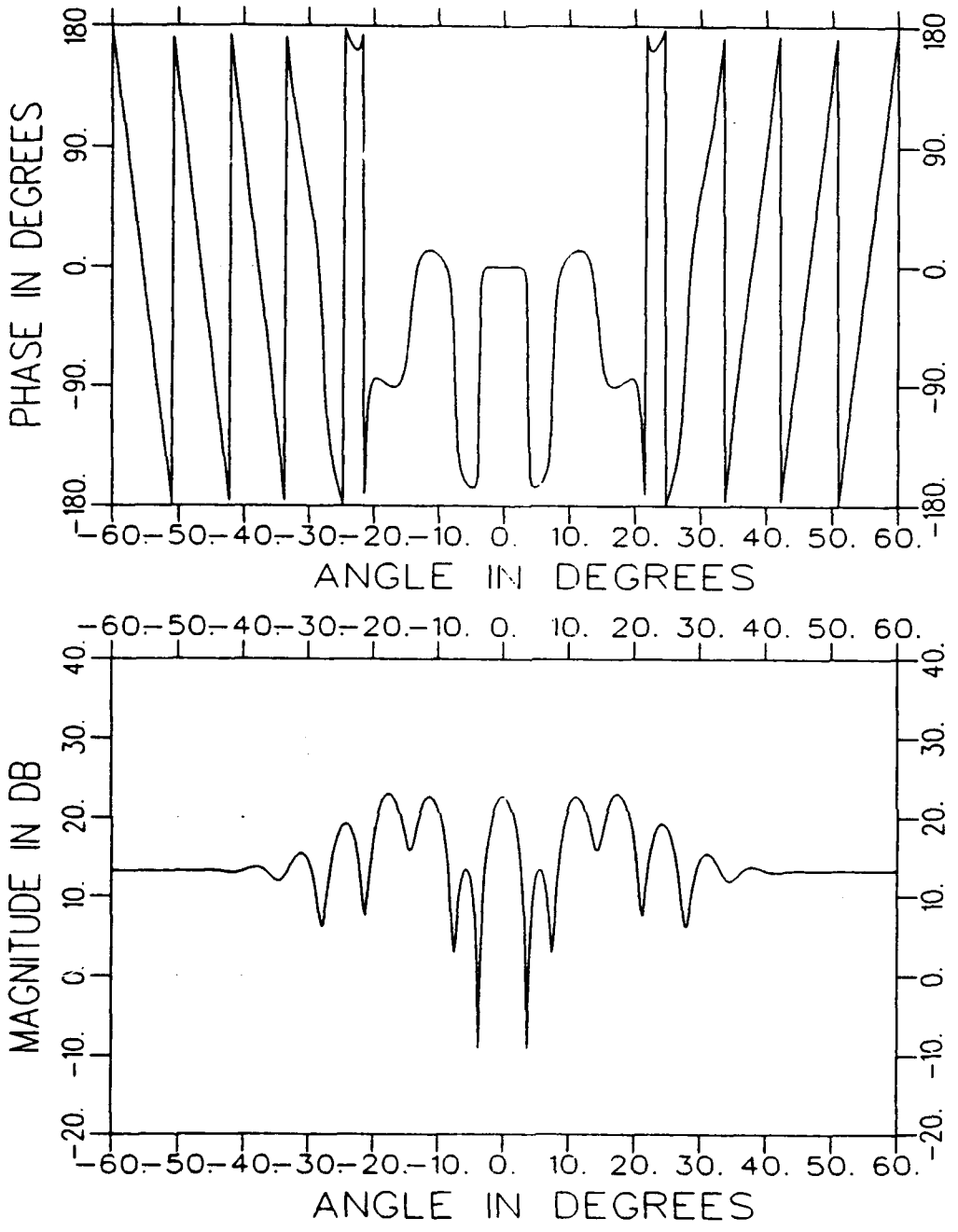

(a) Backscattering by a smoothly indented cavity (Figure 5) of $L = 10.2\lambda$ and $D = 1.25\lambda$.

Figure 9: Backscattering by a smoothly indented cavity (of Figure 5) as well as by a rectangular cavity (of Figure 6).

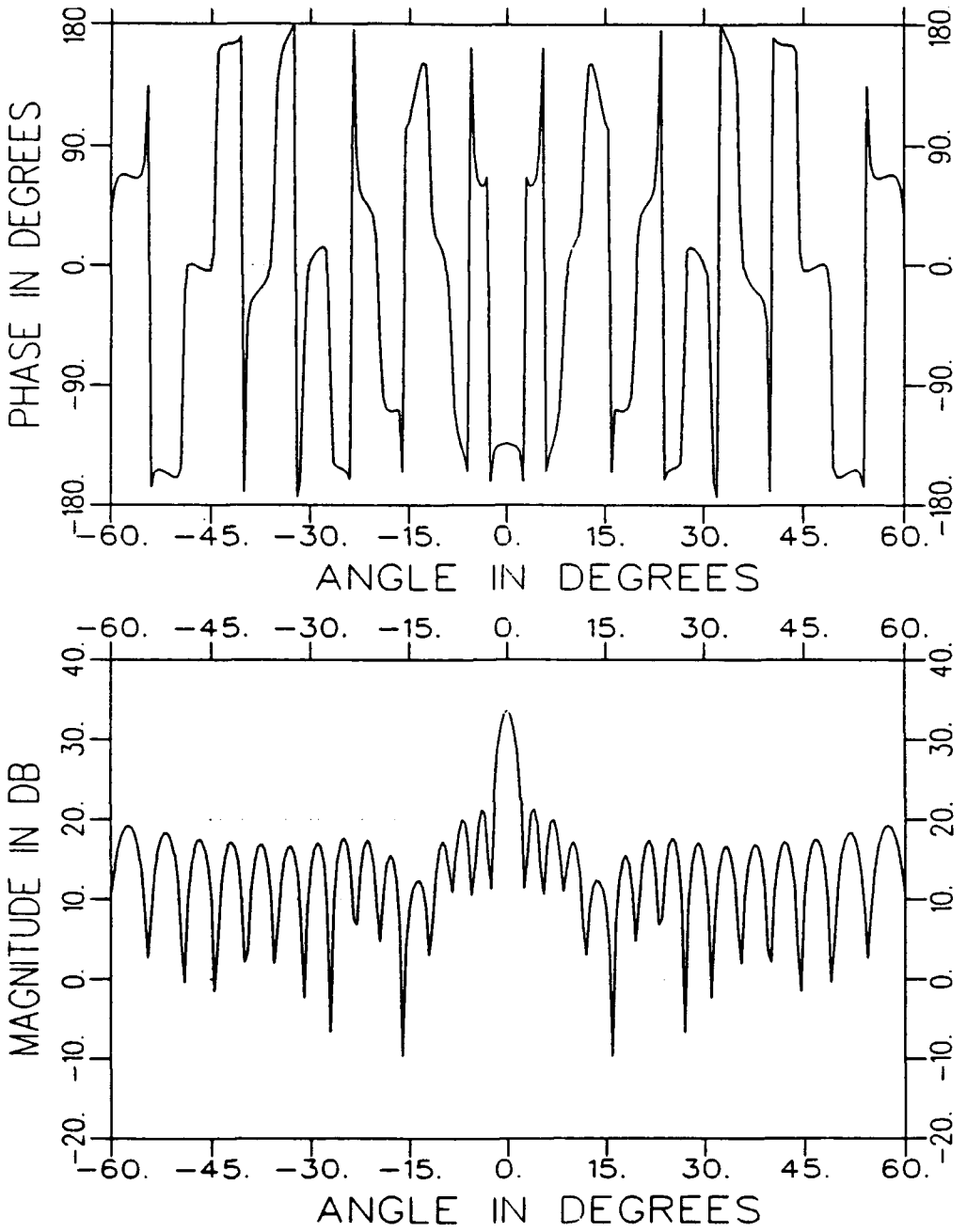

(b) Backscattering by a rectangular cavity (Figure 6) of $L = 10.2\lambda$ and $D = 1.25\lambda$ when the electric field is parallel to the plane of incidence.

Figure 9: (continued)

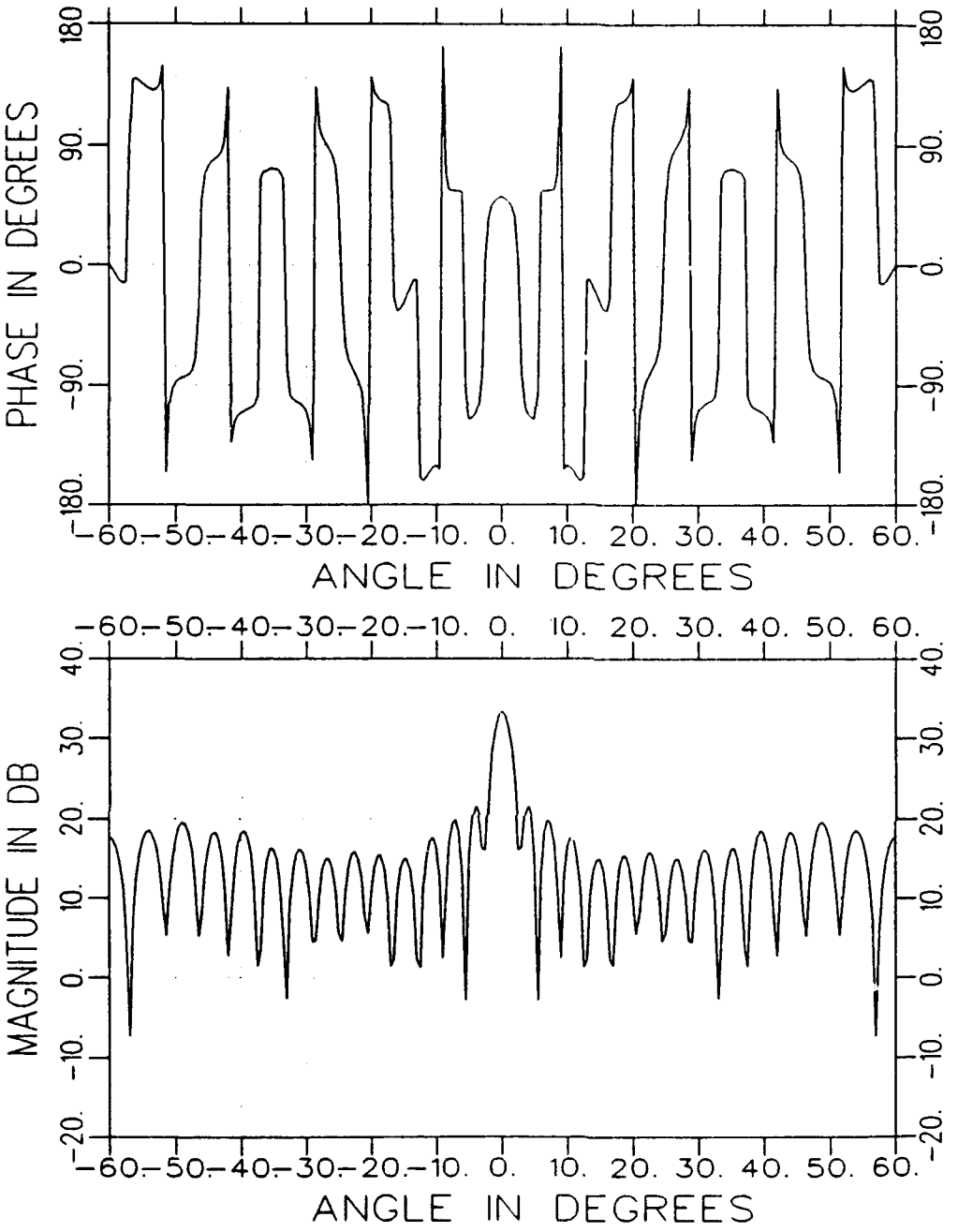

(c) **Backscattering by a rectangular cavity (Figure 6) of $L = 10.2\lambda$ and $D = 1.25\lambda$ when the electric field is perpendicular to the plane of incidence.**

Figure 9: (continued)

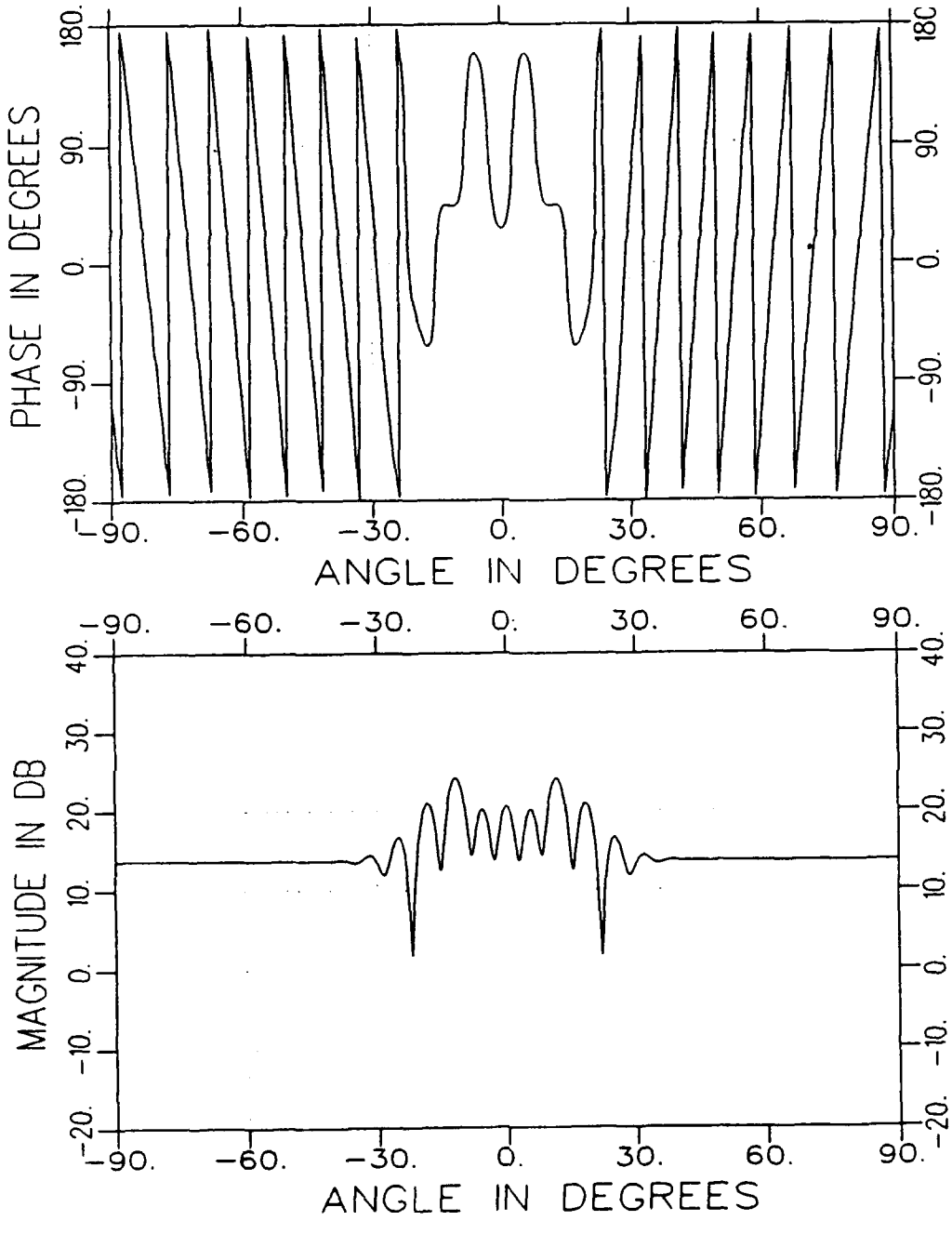

Figure 10: Backscattering by a smoothly indented cavity of Figure 5 with $L = 10.\lambda$ and $D = 1.\lambda$.

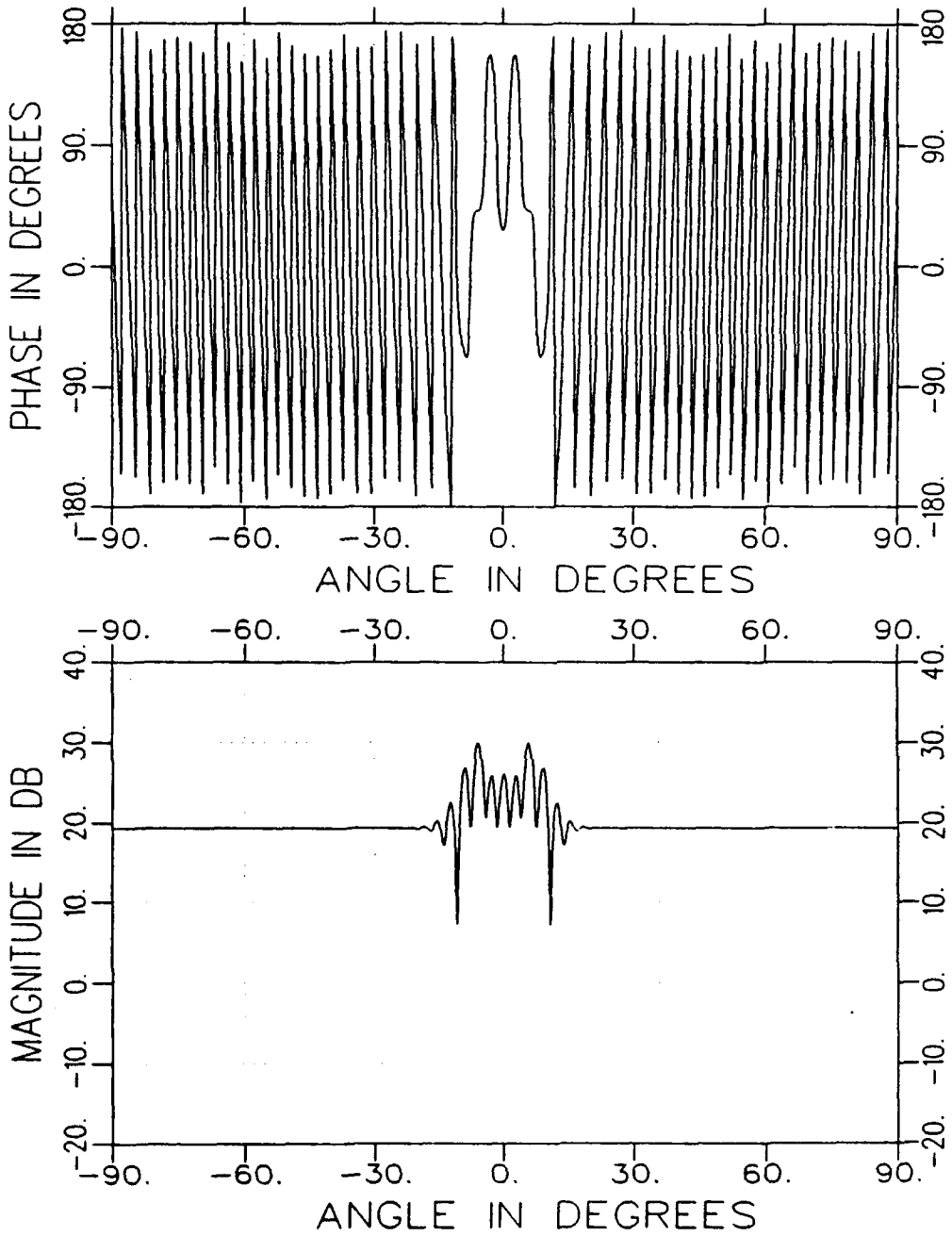

Figure 11: Backscattering by a smoothly indented cavity of Figure 5 with $L = 20.\lambda$ and $D = 1.\lambda$.